AIMS Mathematics, 10(11): 25406–25433.
DOI: 10.3934/math.20251125
Received: 18 May 2025
Revised: 30 July 2025
Accepted: 06 August 2025
Published: 05 November 2025

https://www.aimspress.com/journal/Math

Research article

Fractional order modeling and simulation of a multi-bond orbital chaotic system via Caputo-Fabrizio operators

Elekanyani Madia*, **Anastacia Dlamini, Emile Franc D. Goufo and Melusi Khumalo**

Department of Mathematical Sciences, University of South Africa, Florida Campus, 0003, South Africa

* **Correspondence:** Email: 56678266@mylife.unisa.ac.za.

Abstract: Chaotic systems play a crucial role in science and engineering due to their complex and unpredictable behavior. In this study, we investigated a nonlinear chaotic system known as the multi-bond orbital chaotic attractor (MBOCA), which we modeled using the Caputo Fabrizio fractional operators. We first established the existence and uniqueness of solutions for the system after applying these operators to the MBOCA. We then presented a numerical scheme and analyzed its stability and convergence. To validate the proposed numerical scheme, we performed numerical simulations to visualize the system's behavior for both integer and fractional order cases. The results confirmed that the generated bond-orbital attractors exhibit chaotic behavior, highlighting the influence of fractional order operators on the system's dynamic complexity.

Keywords: chaotic systems; multi-bond orbital chaotic attractor (MBOCA); Caputo–Fabrizio fractional derivative; fractional differential equations; existence and uniqueness; numerical simulation; Adams–Bashforth method
Mathematics Subject Classification: 26A33, 34A08, 34D45, 37D45, 65P20

1. Introduction

Fractional calculus, which generalizes the concepts of differentiation and integration to non-integer orders, has attracted considerable research interest due to its broad applicability in science and engineering [1–4]. It offers a powerful and flexible framework for modeling complex systems with memory effects, hereditary properties, and fractal geometries, and it is particularly well-suited for capturing chaotic dynamics [5–7]. Numerous studies have demonstrated the advantages of fractional calculus over classical integer order models [4, 8–11], with a detailed historical overview provided in [12].

Among the fractional derivatives most studied are the Riemann-Liouville (RL) [13], Caputo-

Fabrizio (CF) [14], and Atangana-Baleanu (AB) [15] operators. The RL derivative, one of the earliest formulations, employs singular-kernel integral operators [1, 16, 17]. In contrast, Caputo and Fabrizio introduced a smooth, non-singular exponential kernel in 2015 [18], and Atangana and Baleanu proposed a non-singular, nonlocal kernel in 2016 [15]. Each of these formulations possesses distinct mathematical characteristics that make them suitable for applications in physics and engineering.

The CF and AB operators have been successfully applied to a range of models, including those involving heat transfer [15] and epidemiological dynamics [19]. For instance, Ahmed et al. [20] employed the AB derivative to model the co-infection dynamics of HIV and COVID-19, demonstrating that fractional operators can significantly improve model accuracy and predictive capabilities. The broad utility of fractional calculus is further evidenced by its growing presence across disciplines [2, 4, 5, 8, 21, 22].

Chaos theory studies nonlinear systems with extreme sensitivity to initial conditions. Although governed by deterministic laws, such systems often behave unpredictably and exhibit complex long-term dynamics [23–27]. Pioneered by Edward Lorenz through a simplified meteorological model, chaos theory revealed how minor variations in initial states could lead to drastically different long-term outcomes [28–32]. Originally developed for weather prediction, chaos theory now finds applications in diverse fields such as medicine [33], chemistry [34], and economics [35]. Notable examples of chaotic systems include the Lorenz system [36–38], the Rössler system [39], Chua's circuit [40], and multiscroll chaotic systems [41].

In recent years, researchers have increasingly explored the interplay between chaos and fractional calculus. For example, Dlamini et al. [42] applied the CF operator to the Lorenz system, developing a numerical scheme and analyzing its behavior under various parameter settings. The same authors later extended this approach to a four-dimensional system with multi-bond orbital chaotic attractors (MBOCA) [43]. Similarly, Saber et al. [44] used the CF operator to stabilize the Burke-Shaw system, demonstrating its effectiveness in controlling complex chaotic dynamics. In another study, Almutairi et al. [45] modeled the Newton-Leipnik system using fractional-order CF derivatives and showed that linear controllers could stabilize its chaotic trajectories, highlighting the advantages of non-singular kernels in chaos control. Additional applications of fractional calculus in chaotic systems can be found in [46–49], collectively emphasizing the potential of fractional-order operators to enhance the modeling, analysis, and stabilization of chaotic dynamics.

Attractors play a fundamental role in the study of chaotic systems, describing the sets toward which a system's trajectory converges over time [50]. They are generally categorized as non-strange, strange non-chaotic, or strange chaotic [34, 50, 51]. Famous examples such as the Hénon, Lorenz, and multiscroll attractors exhibit intricate geometries and strong sensitivity to initial conditions [50, 51]. In particular, multiscroll attractors involve multiple equilibrium points, increasing both their complexity and unpredictability [52, 53]. These characteristics have made them attractive for applications in secure communications and encryption technologies involving images, video, and audio signals [53].

Although fractional calculus has been applied to a variety of chaotic systems, to the best of our knowledge, no prior research has been conducted for the three-dimensional multi-bond orbital chaotic attractor (MBOCA) introduced in [41] using fractional-order CF operators. Zhang et al. [41] examined the MBOCA system in its integer-order form, but its behavior under CF derivatives remains unexplored. This gap in the literature is our primary motivation for this study.

The remainder of the paper is structured as follows. In Section 2, we provide the mathematical

preliminaries. In Section 3, we introduce the three-dimensional chaotic system. In Section 4, we formulate its fractional-order model and establish the existence and uniqueness results. In Section 5, we present the numerical scheme, while in Section 6, we analyze convergence and stability. In Section 7, we provide numerical simulations and graphical representations. In Section 8, we discuss the results and in Section 9, we conclude the paper.

2. Mathematical preliminaries

In this section, we provide the essential definitions and notation for the fractional-order framework used in this paper. Let $\mathbb{R}$ denote the set of real numbers and let $C([0,T],\mathbb{R}^n)$ represent the Banach space of continuous vector-valued functions on $[0,T]$ equipped with the norm

$$\|x\|_\infty := \sup_{t\in[0,T]} \|x(t)\|$$

(see [54]).

Let $T > 0$ be a fixed final time, and let $0 < \psi < 1$ denote the fractional order. We employ the Caputo-Fabrizio (CF) fractional derivative, which has been widely applied due to its non-singular and non-local kernel [15, 18].

2.1. Caputo-Fabrizio fractional derivative

The CF fractional derivative of order ψ of a function $x(t)$ is defined as

$${}^{CF}D_t^{\psi} x(t) = \frac{M(\psi)}{1-\psi}\int_0^t x'(s)\exp\left(-\frac{\psi}{1-\psi}(t-s)\right)ds,$$

where $M(\psi)$ is a normalization function satisfying $M(0) = M(1) = 1$. This operator avoids the singular kernel of classical fractional derivatives and better models memory effects in real-world systems [18, 55].

2.2. Banach fixed-point framework and contraction condition

To prove the existence and uniqueness of solutions, we apply the Banach fixed-point theorem [54]. A mapping $T : X \to X$ is called a contraction if there exists $L \in (0,1)$ such that

$$\|T(x) - T(y)\| \le L\|x - y\|, \quad \forall x, y \in X.$$

Then, T admits a unique fixed point in X.

For the Caputo-Fabrizio fractional system, the contraction condition becomes:

$$\left(1 - \frac{\psi}{M(\psi)}\right)L + \frac{\psi}{M(\psi)}L_T < 1,$$

where L is the Lipschitz constant of the nonlinear function $G(\xi)$, and L_T relates to the time discretization of the system.

This inequality ensures the system remains contractive under fractional dynamics. The memory weight ψ scales the influence of past values, and $M(\psi)$ ensures normalization. Physically, the inequality

means that the system's memory must not overwhelm its local stability. Numerically, it guarantees convergence of the iteration scheme. This type of contraction analysis is commonly used in fractional stability studies [56]. We will apply this contraction principle to the fractional order chaotic system in Section 4.

2.3. Lipschitz continuity

The nonlinear function $G(\xi)$ is defined as

$$G(\xi) = -\xi + f(\xi), \quad f(\xi) = (Q - P) + \sum_{i=1}^{P} \text{sign}\,(\xi + (2i - 1)) + \sum_{j=1}^{Q} \text{sign}\,(\xi - (2j - 1)),$$

and is assumed to be Lipschitz continuous with constant L_G, satisfying

$$\|G(\xi_1) - G(\xi_2)\| \leq L_G \|\xi_1 - \xi_2\|.$$

This guarantees well-posedness for the fractional order formulation [56].

2.4. Notation

We use the standard Euclidean norm $\|\cdot\|$ in $\mathbb{R}^3$ and denote time derivatives with a dot; for example, $\dot{x} = dx/dt$. All fractional derivatives are understood in the Caputo-Fabrizio sense unless otherwise stated. Let $C([0, T], \mathbb{R}^n)$ be the Banach space of continuous vector-valued functions on $[0, T]$, with norm

$$\|x\|_\infty = \sup_{t \in [0,T]} \|x(t)\|,$$

as described in standard functional analysis references [54].

The mapping $G(\xi)$ is defined as

$$G(\xi) = -\xi + f(\xi), \quad f(\xi) = (Q - P) + \sum_{i=1}^{P} \text{sign}\,(\xi + (2i - 1)) + \sum_{j=1}^{Q} \text{sign}\,(\xi - (2j - 1)),$$

and is assumed to satisfy a Lipschitz condition with constant L_G [56].

The contraction constant for the Banach fixed-point theorem is denoted L, and the normalization function for the CF derivative is $M(\psi)$, satisfying $M(0) = M(1) = 1$ [18].

3. The three-dimensional chaotic system

In this section, we introduce the three-dimensional chaotic system considered in this work. The system was originally presented by Zhang et al. [41], and it is defined as follows:

$$\begin{aligned} \dot{\xi} &= r\eta, \\ \dot{\eta} &= s\zeta, \\ \dot{\zeta} &= -\eta - C\zeta + G(\xi, P, Q), \end{aligned} \tag{3.1}$$

where r, s, and C are system parameters with $C \in (0.45, 0.7)$, and s a positive real constant. The variables ξ, η, and ζ represent the state variables. The nonlinear function $G(\xi, P, Q)$ is defined as

$$G(\xi, P, Q) = -\xi + Q - P + \sum_{p=1}^{P} \operatorname{sgn}(\xi + 2p - 1) + \sum_{q=1}^{Q} \operatorname{sgn}(\xi - 2q + 1), \tag{3.2}$$

where P and Q are positive integers used for step adjustment.

4. Existence and uniqueness

In this section, we apply the contraction condition introduced in Section 2 to establish the existence and uniqueness of solutions for the system under the Caputo-Fabrizio fractional derivative. We adopt the approach presented in [14]. The fractional order formulation is given by:

$$\begin{aligned} {}_0^{CF}D_t^{\psi}\xi(\tau) &= \mathscr{F}_1(\xi, \eta, \zeta, \tau), \\ {}_0^{CF}D_t^{\psi}\eta(\tau) &= \mathscr{F}_2(\xi, \eta, \zeta, \tau), \\ {}_0^{CF}D_t^{\psi}\zeta(\tau) &= \mathscr{F}_3(\xi, \eta, \zeta, \tau), \end{aligned} \tag{4.1}$$

with the initial conditions:

$$\xi(\tau_0) = \xi_0, \quad \eta(\tau_0) = \eta_0, \quad \zeta(\tau_0) = \zeta_0.$$

The functions on the right-hand side are defined as

$$\mathscr{F}_1(\xi, \eta, \zeta, \tau) = r\eta, \quad \mathscr{F}_2(\xi, \eta, \zeta, \tau) = s\zeta, \quad \mathscr{F}_3(\xi, \eta, \zeta, \tau) = -\eta - C\zeta + G(\xi, P, Q).$$

In integral form, these equations become:

$$\begin{aligned} \frac{M(\psi)}{1-\psi}\int_0^t \xi'(\sigma)\exp\left(\frac{-\psi}{1-\psi}(t-\sigma)\right)d\sigma &= \mathscr{F}_1(\xi, \eta, \zeta, \tau), \\ \frac{M(\psi)}{1-\psi}\int_0^t \eta'(\sigma)\exp\left(\frac{-\psi}{1-\psi}(t-\sigma)\right)d\sigma &= \mathscr{F}_2(\xi, \eta, \zeta, \tau), \\ \frac{M(\psi)}{1-\psi}\int_0^t \zeta'(\sigma)\exp\left(\frac{-\psi}{1-\psi}(t-\sigma)\right)d\sigma &= \mathscr{F}_3(\xi, \eta, \zeta, \tau). \end{aligned} \tag{4.2}$$

By applying the fundamental theorem of calculus, we obtain the following expressions:

$$\begin{aligned} \xi(\tau) &= \xi(0) + \frac{1-\psi}{M(\psi)}\mathscr{F}_1(\xi, \eta, \zeta, \tau) + \frac{\psi}{M(\psi)}\int_0^t \mathscr{F}_1(\xi, \eta, \zeta, \sigma)d\sigma, \\ \eta(\tau) &= \eta(0) + \frac{1-\psi}{M(\psi)}\mathscr{F}_2(\xi, \eta, \zeta, \tau) + \frac{\psi}{M(\psi)}\int_0^t \mathscr{F}_2(\xi, \eta, \zeta, \sigma)d\sigma, \\ \zeta(\tau) &= \zeta(0) + \frac{1-\psi}{M(\psi)}\mathscr{F}_3(\xi, \eta, \zeta, \tau) + \frac{\psi}{M(\psi)}\int_0^t \mathscr{F}_3(\xi, \eta, \zeta, \sigma)d\sigma. \end{aligned} \tag{4.3}$$

We define the operators T_1, T_2, and T_3 acting on functions $\xi(\tau)$, $\eta(\tau)$, and $\zeta(\tau)$, respectively, as:

$$\begin{aligned}
(T_1\xi)(\tau) &= \xi_0 + \frac{1-\psi}{M(\psi)}\mathscr{F}_1(\xi,\eta,\zeta,\tau) + \frac{\psi}{M(\psi)}\int_0^t \mathscr{F}_1(\xi,\eta,\zeta,\sigma)d\sigma,\\
(T_2\eta)(\tau) &= \eta_0 + \frac{1-\psi}{M(\psi)}\mathscr{F}_2(\xi,\eta,\zeta,\tau) + \frac{\psi}{M(\psi)}\int_0^t \mathscr{F}_2(\xi,\eta,\zeta,\sigma)d\sigma,\\
(T_3\zeta)(\tau) &= \zeta_0 + \frac{1-\psi}{M(\psi)}\mathscr{F}_3(\xi,\eta,\zeta,\tau) + \frac{\psi}{M(\psi)}\int_0^t \mathscr{F}_3(\xi,\eta,\zeta,\sigma)d\sigma.
\end{aligned} \tag{4.4}$$

We aim to show that T_1, T_2, and T_3 are contraction mappings in the Banach space of continuous functions $C([0,T])$ with the norm

$$\|\xi\|_\infty = \sup_{\tau\in[0,T]} |\xi(\tau)|.$$

To apply the Banach fixed-point theorem, we verify the Lipschitz condition:

$$\|\mathscr{G}(\Lambda_1) - \mathscr{G}(\Lambda_2)\| \le L\|\Lambda_1 - \Lambda_2\|$$

for some Lipschitz constant $L > 0$, where $\Lambda = (\xi,\eta,\zeta)$, and $\mathscr{G}(\Lambda)$ is defined as:

$$\mathscr{G}(\Lambda) = \begin{bmatrix} r\eta \\ s\zeta \\ -\eta - C\zeta + G(\xi,P,Q) \end{bmatrix}.$$

For each component, we verify:

$$|r\eta_1 - r\eta_2| = |r|\,|\eta_1 - \eta_2| \Rightarrow L_1 = |r|,$$

$$|s\zeta_1 - s\zeta_2| = |s|\,|\zeta_1 - \zeta_2| \Rightarrow L_2 = |s|.$$

For the third component:

$$\begin{aligned}
&|(-\eta_1 - C\zeta_1 + G(\xi_1,P,Q)) - (-\eta_2 - C\zeta_2 + G(\xi_2,P,Q))|\\
&\le |\eta_1 - \eta_2| + |C||\zeta_1 - \zeta_2| + |G(\xi_1,P,Q) - G(\xi_2,P,Q)|,
\end{aligned}$$

where the function $G(\xi,P,Q)$ includes sign functions. Since $\mathrm{sgn}(\cdot)$ is piecewise constant, $G(\xi)$ is Lipschitz with:

$$|G(\xi_1) - G(\xi_2)| \le 2(P+Q) \Rightarrow L_G \le 2(P+Q).$$

Hence,

$$L_3 = \max(1, |C|, L_G).$$

Applying the contraction condition, for T_1:

$$\|T_1\xi_1 - T_1\xi_2\| \le \left(\frac{1-\psi}{M(\psi)}L_1 + \frac{\psi}{M(\psi)}L_1T\right)\|\eta_1 - \eta_2\|.$$

Similarly, for T_2:

$$\|T_2\eta_1 - T_2\eta_2\| \le \left(\frac{1-\psi}{M(\psi)}L_2 + \frac{\psi}{M(\psi)}L_2T\right)\|\zeta_1 - \zeta_2\|.$$

Additionally, for T_3:

$$\|T_3\zeta_1 - T_3\zeta_2\| \leq \left(\frac{1-\psi}{M(\psi)}L_3 + \frac{\psi}{M(\psi)}L_3T\right)(\|\eta_1 - \eta_2\| + \|\zeta_1 - \zeta_2\|).$$

Thus, the combined contraction condition is:

$$\frac{1-\psi}{M(\psi)}L + \frac{\psi}{M(\psi)}LT < 1.$$

Therefore, the operators T_1, T_2, and T_3 satisfy the contraction mapping principle, confirming the existence and uniqueness of the solution using the Banach fixed-point theorem.

5. Numerical scheme

In this section, we present a numerical scheme for solving fractional order differential equations based on the Caputo-Fabrizio fractional derivative. To achieve this, we transform the equations in (4.2) by applying the fundamental theorem of calculus, following the method outlined in [14], to obtain:

$$\begin{aligned}
\xi(\tau) - \xi(0) &= \frac{1-\psi}{M(\psi)}\mathscr{F}_1(\xi,\eta,\zeta,\tau) + \frac{\psi}{M(\psi)}\int_0^\tau \mathscr{F}_1(\xi,\eta,\zeta,\sigma)\,d\sigma,\\
\eta(\tau) - \eta(0) &= \frac{1-\psi}{M(\psi)}\mathscr{F}_2(\xi,\eta,\zeta,\tau) + \frac{\psi}{M(\psi)}\int_0^\tau \mathscr{F}_2(\xi,\eta,\zeta,\sigma)\,d\sigma,\\
\zeta(\tau) - \zeta(0) &= \frac{1-\psi}{M(\psi)}\mathscr{F}_3(\xi,\eta,\zeta,\tau) + \frac{\psi}{M(\psi)}\int_0^\tau \mathscr{F}_3(\xi,\eta,\zeta,\sigma)\,d\sigma.
\end{aligned} \tag{5.1}$$

At τ_{n+1}, we obtain:

$$\begin{aligned}
\xi(\tau_{n+1}) - \xi(0) &= \frac{1-\psi}{M(\psi)}\mathscr{F}_1(\xi_n,\eta_n,\zeta_n,\tau_n) + \frac{\psi}{M(\psi)}\int_0^{\tau_{n+1}} \mathscr{F}_1(\xi,\eta,\zeta,\tau)\,d\tau,\\
\eta(\tau_{n+1}) - \eta(0) &= \frac{1-\psi}{M(\psi)}\mathscr{F}_2(\xi_n,\eta_n,\zeta_n,\tau_n) + \frac{\psi}{M(\psi)}\int_0^{\tau_{n+1}} \mathscr{F}_2(\xi,\eta,\zeta,\tau)\,d\tau,\\
\zeta(\tau_{n+1}) - \zeta(0) &= \frac{1-\psi}{M(\psi)}\mathscr{F}_3(\xi_n,\eta_n,\zeta_n,\tau_n) + \frac{\psi}{M(\psi)}\int_0^{\tau_{n+1}} \mathscr{F}_3(\xi,\eta,\zeta,\tau)\,d\tau.
\end{aligned} \tag{5.2}$$

Similarly, at τ_n, we have:

$$\begin{aligned}
\xi(\tau_n) - \xi(0) &= \frac{1-\psi}{M(\psi)}\mathscr{F}_1(\xi_{n-1},\eta_{n-1},\zeta_{n-1},\tau_{n-1}) + \frac{\psi}{M(\psi)}\int_0^{\tau_n} \mathscr{F}_1(\xi,\eta,\zeta,\tau)\,d\tau,\\
\eta(\tau_n) - \eta(0) &= \frac{1-\psi}{M(\psi)}\mathscr{F}_2(\xi_{n-1},\eta_{n-1},\zeta_{n-1},\tau_{n-1}) + \frac{\psi}{M(\psi)}\int_0^{\tau_n} \mathscr{F}_2(\xi,\eta,\zeta,\tau)\,d\tau,\\
\zeta(\tau_n) - \zeta(0) &= \frac{1-\psi}{M(\psi)}\mathscr{F}_3(\xi_{n-1},\eta_{n-1},\zeta_{n-1},\tau_{n-1}) + \frac{\psi}{M(\psi)}\int_0^{\tau_n} \mathscr{F}_3(\xi,\eta,\zeta,\tau)\,d\tau.
\end{aligned} \tag{5.3}$$

Subtracting the two equations yields:

$$\xi(\tau_{n+1}) - \xi(\tau_n) = \frac{1-\psi}{M(\psi)}\left[\mathscr{F}_1(\xi_n,\eta_n,\zeta_n,\tau_n) - \mathscr{F}_1(\xi_{n-1},\eta_{n-1},\zeta_{n-1},\tau_{n-1})\right]$$

$$
\begin{aligned}
&+\frac{\psi}{M(\psi)}\int_{\tau_n}^{\tau_{n+1}}\mathscr{F}_1(\xi,\eta,\zeta,\tau)\,d\tau,\\
\eta(\tau_{n+1})-\eta(\tau_n)&=\frac{1-\psi}{M(\psi)}\left[\mathscr{F}_2(\xi_n,\eta_n,\zeta_n,\tau_n)-\mathscr{F}_2(\xi_{n-1},\eta_{n-1},\zeta_{n-1},\tau_{n-1})\right]\\
&+\frac{\psi}{M(\psi)}\int_{\tau_n}^{\tau_{n+1}}\mathscr{F}_2(\xi,\eta,\zeta,\tau)\,d\tau,\\
\zeta(\tau_{n+1})-\zeta(\tau_n)&=\frac{1-\psi}{M(\psi)}\left[\mathscr{F}_3(\xi_n,\eta_n,\zeta_n,\tau_n)-\mathscr{F}_3(\xi_{n-1},\eta_{n-1},\zeta_{n-1},\tau_{n-1})\right]\\
&+\frac{\psi}{M(\psi)}\int_{\tau_n}^{\tau_{n+1}}\mathscr{F}_3(\xi,\eta,\zeta,\tau)\,d\tau.
\end{aligned}\tag{5.4}
$$

The integral terms are given by:

$$
\begin{aligned}
\int_{\tau_n}^{\tau_{n+1}}\mathscr{F}_1(\xi,\eta,\zeta,\tau)\,d\tau&\approx\frac{3h}{2}\mathscr{F}_1(\xi_n,\eta_n,\zeta_n,\tau_n)-\frac{h}{2}\mathscr{F}_1(\xi_{n-1},\eta_{n-1},\zeta_{n-1},\tau_{n-1}),\\
\int_{\tau_n}^{\tau_{n+1}}\mathscr{F}_2(\xi,\eta,\zeta,\tau)\,d\tau&\approx\frac{3h}{2}\mathscr{F}_2(\xi_n,\eta_n,\zeta_n,\tau_n)-\frac{h}{2}\mathscr{F}_2(\xi_{n-1},\eta_{n-1},\zeta_{n-1},\tau_{n-1}),\\
\int_{\tau_n}^{\tau_{n+1}}\mathscr{F}_3(\xi,\eta,\zeta,\tau)\,d\tau&\approx\frac{3h}{2}\mathscr{F}_3(\xi_n,\eta_n,\zeta_n,\tau_n)-\frac{h}{2}\mathscr{F}_3(\xi_{n-1},\eta_{n-1},\zeta_{n-1},\tau_{n-1}).
\end{aligned}\tag{5.5}
$$

Thus, we obtain:

$$
\begin{aligned}
\xi(\tau_{n+1})-\xi(\tau_n)&=\frac{1-\psi}{M(\psi)}\left[\mathscr{F}_1(\xi_n,\eta_n,\zeta_n,\tau_n)-\mathscr{F}_1(\xi_{n-1},\eta_{n-1},\zeta_{n-1},\tau_{n-1})\right]\\
&+\frac{3\psi h}{2M(\psi)}\mathscr{F}_1(\xi_n,\eta_n,\zeta_n,\tau_n)-\frac{\psi h}{2M(\psi)}\mathscr{F}_1(\xi_{n-1},\eta_{n-1},\zeta_{n-1},\tau_{n-1}),\\
\eta(\tau_{n+1})-\eta(\tau_n)&=\frac{1-\psi}{M(\psi)}\left[\mathscr{F}_2(\xi_n,\eta_n,\zeta_n,\tau_n)-\mathscr{F}_2(\xi_{n-1},\eta_{n-1},\zeta_{n-1},\tau_{n-1})\right]\\
&+\frac{3\psi h}{2M(\psi)}\mathscr{F}_2(\xi_n,\eta_n,\zeta_n,\tau_n)-\frac{\psi h}{2M(\psi)}\mathscr{F}_2(\xi_{n-1},\eta_{n-1},\zeta_{n-1},\tau_{n-1}),\\
\zeta(\tau_{n+1})-\zeta(\tau_n)&=\frac{1-\psi}{M(\psi)}\left[\mathscr{F}_3(\xi_n,\eta_n,\zeta_n,\tau_n)-\mathscr{F}_3(\xi_{n-1},\eta_{n-1},\zeta_{n-1},\tau_{n-1})\right]\\
&+\frac{3\psi h}{2M(\psi)}\mathscr{F}_3(\xi_n,\eta_n,\zeta_n,\tau_n)-\frac{\psi h}{2M(\psi)}\mathscr{F}_3(\xi_{n-1},\eta_{n-1},\zeta_{n-1},\tau_{n-1}).
\end{aligned}\tag{5.6}
$$

Hence, the numerical scheme is derived as:

$$
\begin{aligned}
\xi_{n+1}&=\xi_n+A\mathscr{F}_1(\xi_n,\eta_n,\zeta_n,\tau_n)+B\mathscr{F}_1(\xi_{n-1},\eta_{n-1},\zeta_{n-1},\tau_{n-1}),\\
\eta_{n+1}&=\eta_n+A\mathscr{F}_2(\xi_n,\eta_n,\zeta_n,\tau_n)+B\mathscr{F}_2(\xi_{n-1},\eta_{n-1},\zeta_{n-1},\tau_{n-1}),\\
\zeta_{n+1}&=\zeta_n+A\mathscr{F}_3(\xi_n,\eta_n,\zeta_n,\tau_n)+B\mathscr{F}_3(\xi_{n-1},\eta_{n-1},\zeta_{n-1},\tau_{n-1}),
\end{aligned}\tag{5.7}
$$

where

$$
A=\frac{1-\psi}{M(\psi)}+\frac{3\psi h}{2M(\psi)},\quad B=-\left(\frac{1-\psi}{M(\psi)}+\frac{\psi h}{2M(\psi)}\right).
$$

We obtain a two-step Adams-Bashforth scheme for approximating the solutions of fractional order differential systems involving the Caputo-Fabrizio derivative.

6. Convergence and stability results

In this section, we examine the stability and convergence of the numerical scheme introduced in Section 5.

Let $\xi(\tau)$, $\eta(\tau)$ and $\zeta(\tau)$ be a solution of ${}_0^{CF}D_t^{\psi}\xi(\tau) = \mathscr{F}_1(\xi,\eta,\zeta,\tau)$, ${}_0^{CF}D_t^{\psi}\eta(\tau) = \mathscr{F}_2(\xi,\eta,\zeta,\tau)$ and ${}_0^{CF}D_t^{\psi}\zeta(\tau) = \mathscr{F}_3(\xi,\eta,\zeta,\tau)$ where $\mathscr{F}_1$, $\mathscr{F}_2$ and $\mathscr{F}_3$ are continuous functions bounded for the Caputo-Fabrizio fractional derivatives, respectively, we have

$$\begin{aligned}
\xi_{n+1} &= \xi_n + \Big(\frac{1-\psi}{M(\psi)} + \frac{3\psi h}{2M(\psi)}\Big)\mathscr{F}_1(\xi_n,\eta_n,\zeta_n,\tau_n) \\
&\quad + \Big(\frac{1-\psi}{M(\psi)} + \frac{\psi h}{2M(\psi)}\Big)\mathscr{F}_1(\xi_{n-1},\eta_{n-1},\zeta_{n-1},\tau_{n-1}) + R^n_{1,\psi} \\
\eta_{n+1} &= \eta_n + \Big(\frac{1-\psi}{M(\psi)} + \frac{3\psi h}{2M(\psi)}\Big)\mathscr{F}_2(\xi_n,\eta_n,\zeta_n,\tau_n) \\
&\quad + \Big(\frac{1-\psi}{M(\psi)} + \frac{\psi h}{2M(\psi)}\Big)\mathscr{F}_2(\xi_{n-1},\eta_{n-1},\zeta_{n-1},\tau_{n-1}) + R^n_{2,\psi} \\
\zeta_{n+1} &= \zeta_n + \Big(\frac{1-\psi}{M(\psi)} + \frac{3\psi h}{2M(\psi)}\Big)\mathscr{F}_3(\xi_n,\eta_n,\zeta_n,\tau_n) \\
&\quad + \Big(\frac{1-\psi}{M(\psi)} + \frac{\psi h}{2M(\psi)}\Big)\mathscr{F}_3(\xi_{n-1},\eta_{n-1},\zeta_{n-1},\tau_{n-1}) + R^n_{3,\psi}
\end{aligned} \tag{6.1}$$

where $\|R^n_{1,\psi}\| \le M$, $\|R^n_{2,\psi}\| \le M$, and $\|R^n_{3,\psi}\| \le M$.

According to the definition of the Caputo-Fabrizio, we have

$$\begin{aligned}
\xi(\tau) - \xi(0) &= \frac{1-\psi}{M(\psi)}\mathscr{F}_1(\xi,\eta,\zeta,\tau) + \frac{\psi}{M(\psi)}\int_0^{\tau}\mathscr{F}_1(\xi,\eta,\zeta,\sigma)d\sigma \\
\eta(\tau) - \eta(0) &= \frac{1-\psi}{M(\psi)}\mathscr{F}_2(\xi,\eta,\zeta,\tau) + \frac{\psi}{M(\psi)}\int_0^{\tau}\mathscr{F}_2(\xi,\eta,\zeta,\sigma)d\sigma \\
\zeta(\tau) - \zeta(0) &= \frac{1-\psi}{M(\psi)}\mathscr{F}_3(\xi,\eta,\zeta,\tau) + \frac{\psi}{M(\psi)}\int_0^{\tau}\mathscr{F}_3(\xi,\eta,\zeta,\sigma)d\sigma.
\end{aligned} \tag{6.2}$$

At τ_{n+1}, we get

$$\begin{aligned}
\xi(\tau_{n+1}) &= \frac{1-\psi}{M(\psi)}\mathscr{F}_1(\xi_n,\eta_n,\zeta_n,\tau_n) + \frac{\psi}{M(\psi)}\int_0^{\tau_{n+1}}\mathscr{F}_1(\xi,\eta,\zeta,\tau)d\tau \\
\eta(\tau_{n+1}) &= \frac{1-\psi}{M(\psi)}\mathscr{F}_2(\xi_n,\eta_n,\zeta_n,\tau_n) + \frac{\psi}{M(\psi)}\int_0^{\tau_{n+1}}\mathscr{F}_2(\xi,\eta,\zeta,\tau)d\tau \\
\zeta(\tau_{n+1}) &= \frac{1-\psi}{M(\psi)}\mathscr{F}_3(\xi_n,\eta_n,\zeta_n,\tau_n) + \frac{\psi}{M(\psi)}\int_0^{\tau_{n+1}}\mathscr{F}_3(\xi,\eta,\zeta,\tau)d\tau
\end{aligned} \tag{6.3}$$

and at τ_n , we have

$$\begin{aligned}
\xi(\tau_n) &= \frac{1-\psi}{M(\psi)}\mathscr{F}_1(\xi_{n-1},\eta_{n-1},\zeta_{n-1},\tau_{n-1}) + \frac{\psi}{M(\psi)}\int_0^{\tau_n}\mathscr{F}_1(\xi,\eta,\zeta,\tau)d\tau \\
\eta(\tau_n) &= \frac{1-\psi}{M(\psi)}\mathscr{F}_2(\xi_{n-1},\eta_{n-1},\zeta_{n-1},\tau_{n-1}) + \frac{\psi}{M(\psi)}\int_0^{\tau_n}\mathscr{F}_2(\xi,\eta,\zeta,\tau)d\tau
\end{aligned} \tag{6.4}$$

$$\zeta(\tau_n) = \frac{1-\psi}{M(\psi)}\mathscr{F}_3(\xi_{n-1}, \eta_{n-1}, \zeta_{n-1}, \tau_{n-1}) + \frac{\psi}{M(\psi)}\int_0^{\tau_n} \mathscr{F}_3(\xi, \eta, \zeta, \tau)d\tau.$$

Thus,

$$\begin{aligned}
\xi(\tau_{n+1}) - \xi(\tau_n) &= \frac{1-\psi}{M(\psi)}\left[\mathscr{F}_1(\xi_n, \eta_n, \zeta_n, \tau_n) - \mathscr{F}_1(\xi_{n-1}, \eta_{n-1}, \zeta_{n-1}, \tau_{n-1})\right] \\
&+ \frac{\psi}{M(\psi)}\int_{\tau_n}^{\tau_{n+1}} \mathscr{F}_1(\xi, \eta, \zeta, \tau)d\tau \\
&= \frac{1-\psi}{M(\psi)}\left[\mathscr{F}_1(\xi_n, \eta_n, \zeta_n, \tau_n) - \mathscr{F}_1(\xi_{n-1}, \eta_{n-1}, \zeta_{n-1})\right] \\
&+ \frac{\psi}{M(\psi)}\Big\{\frac{\mathscr{F}_1(\xi_n, \eta_n, \zeta_n, \tau_n)}{h}(\tau - \tau_{n-1}) \\
&- \frac{\mathscr{F}_1(\xi_{n-1}, \eta_{n-1}, \zeta_{n-1}, \tau_{n-1})}{h}(\tau - \tau_n) + \sum_{i=2}^{n}\prod_{i=2}^{n}\frac{(\tau - \tau_i)}{h(-1)^i}\mathscr{F}_1(\xi_i, \eta_i, \zeta_i, \tau_i)\Big\}d\tau \\
\eta(\tau_{n+1}) - \eta(\tau_n) &= \frac{1-\psi}{M(\psi)}\left[\mathscr{F}_2(\xi_n, \eta_n, \zeta_n, \tau_n) - \mathscr{F}_2(\xi_{n-1}, \eta_{n-1}, \zeta_{n-1}, \tau_{n-1})\right] \\
&+ \frac{\psi}{M(\psi)}\int_{\tau_n}^{\tau_{n+1}} \mathscr{F}_2(\xi, \eta, \zeta, \tau)d\tau \\
&= \frac{1-\psi}{M(\psi)}\left[\mathscr{F}_2(\xi_n, \eta_n, \zeta_n, \tau_n) - \mathscr{F}_2(\xi_{n-1}, \eta_{n-1}, \zeta_{n-1})\right] \\
&+ \frac{\psi}{M(\psi)}\Big\{\frac{\mathscr{F}_2(\xi_n, \eta_n, \zeta_n, \tau_n)}{h}(\tau - \tau_{n-1}) \\
&- \frac{\mathscr{F}_2(\xi_{n-1}, \eta_{n-1}, \zeta_{n-1}, \tau_{n-1})}{h}(\tau - \tau_n) + \sum_{i=2}^{n}\prod_{i=2}^{n}\frac{(\tau - \tau_i)}{h(-1)^i}\mathscr{F}_2(\xi_i, \eta_i, \zeta_i, \tau_i)\Big\}d\tau
\end{aligned}$$

$$\begin{aligned}
\zeta(\tau_{n+1}) - \zeta(\tau_n) &= \frac{1-\psi}{M(\psi)}\left[\mathscr{F}_3(\xi_n, \eta_n, \zeta_n, \tau_n) - \mathscr{F}_3(\xi_{n-1}, \eta_{n-1}, \zeta_{n-1}, \tau_{n-1})\right] \\
&+ \frac{\psi}{M(\psi)}\int_{\tau_n}^{\tau_{n+1}} \mathscr{F}_3(\xi, \eta, \zeta, \tau)d\tau \\
&= \frac{1-\psi}{M(\psi)}\left[\mathscr{F}_3(\xi_n, \eta_n, \zeta_n, \tau_n) - \mathscr{F}_3(\xi_{n-1}, \eta_{n-1}, \zeta_{n-1})\right] \\
&+ \frac{\psi}{M(\psi)}\Big\{\frac{\mathscr{F}_3(\xi_n, \eta_n, \zeta_n, \tau_n)}{h}(\tau - \tau_{n-1}) \\
&- \frac{\mathscr{F}_1(\xi_{n-1}, \eta_{n-1}, \zeta_{n-1}, \tau_{n-1})}{h}(\tau - \tau_n) + \sum_{i=2}^{n}\prod_{i=2}^{n}\frac{(\tau - \tau_i)}{h(-1)^i}\mathscr{F}_3(\xi_i, \eta_i, \zeta_i, \tau_i)\Big\}d\tau
\end{aligned} \tag{6.5}$$

so that

$$\begin{aligned}
\xi_{n+1} &= \xi_n + \Big(\frac{1-\psi}{M(\psi)} + \frac{3\psi h}{2M(\psi)}\Big)\mathscr{F}_1(\xi_n, \eta_n, \zeta_n, \tau_n) + \Big(\frac{1-\psi}{M(\psi)} + \frac{\psi h}{2M(\psi)}\Big)\mathscr{F}_1(\xi_{n-1}, \eta_{n-1}, \zeta_{n-1}, \tau_{n-1}) \\
&+ \frac{\psi}{M(\psi)}\int_{\tau_n}^{\tau_{n+1}} \sum_{i=2}^{n}\prod_{i=2}^{n}\frac{(\tau - \tau_i)}{h(-1)^i}\mathscr{F}_1(\xi_i, \eta_i, \zeta_i, \tau_i)d\tau
\end{aligned}$$

$$\eta_{n+1} = \eta_n + \Big(\frac{1-\psi}{M(\psi)} + \frac{3\psi h}{2M(\psi)}\Big)\mathscr{F}_2(\xi_n, \eta_n, \zeta_n, \tau_n)\Big(\frac{1-\psi}{M(\psi)} + \frac{\psi h}{2M(\psi)}\Big)\mathscr{F}_2(\xi_{n-1}, \eta_{n-1}, \zeta_{n-1}, \tau_{n-1}) \tag{6.6}$$
$$+ \frac{\psi}{M(\psi)}\int_{\tau_n}^{\tau_{n+1}} \sum_{i=2}^{n}\prod_{i=2}^{n}\frac{(\tau-\tau_i)}{h(-1)^i}\mathscr{F}_2(\xi_i, \eta_i, \zeta_i, \tau_i)d\tau$$
$$\zeta_{n+1} = \zeta_n + \Big(\frac{1-\psi}{M(\psi)} + \frac{3\psi h}{2M(\psi)}\Big)\mathscr{F}_3(\xi_n, \eta_n, \zeta_n, \tau_n) + \Big(\frac{1-\psi}{M(\psi)} + \frac{\psi h}{2M(\psi)}\Big)\mathscr{F}_3(\xi_{n-1}, \eta_{n-1}, \zeta_{n-1}, \tau_{n-1})$$
$$+ \frac{\psi}{M(\psi)}\int_{\tau_n}^{\tau_{n+1}} \sum_{i=2}^{n}\prod_{i=2}^{n}\frac{(\tau-\tau_i)}{h(-1)^i}\mathscr{F}_3(\xi_i, \eta_i, \zeta_i, \tau_i)d\tau.$$

We denote the error terms by

$$R^n_{1,\psi} = \frac{\psi}{M(\psi)}\int_{\tau_n}^{\tau_{n+1}} \sum_{i=2}^{n}\prod_{i=2}^{n}\frac{(\tau-\tau_i)}{h(-1)^i}\mathscr{F}_1(\xi_i, \eta_i, \zeta_i, \tau_i)d\tau$$
$$R^n_{2,\psi} = \frac{\psi}{M(\psi)}\int_{\tau_n}^{\tau_{n+1}} \sum_{i=2}^{n}\prod_{i=2}^{n}\frac{(\tau-\tau_i)}{h(-1)^i}\mathscr{F}_2(\xi_i, \eta_i, \zeta_i, \tau_i)d\tau$$
$$R^n_{3,\psi} = \frac{\psi}{M(\psi)}\int_{\tau_n}^{\tau_{n+1}} \sum_{i=2}^{n}\prod_{i=2}^{n}\frac{(\tau-\tau_i)}{h(-1)^i}\mathscr{F}_3(\xi_i, \eta_i, \zeta_i, \tau_i)d\tau.$$

Thus,

$$\begin{aligned}
\|R^n_{1,\psi}\|_\infty &= \frac{\psi}{M(\psi)}\Big\|\int_{\tau_n}^{\tau_{n+1}} \sum_{i=2}^{n}\prod_{i=2}^{n}\frac{(\tau-\tau_i)}{h(-1)^i}\mathscr{F}_1(\xi_i, \eta_i, \zeta_i, \tau_i)d\tau\Big\|_\infty \\
&\leq \frac{\psi}{M(\psi)}\int_{\tau_n}^{\tau_{n+1}} \Big\|\sum_{i=2}^{n}\prod_{i=2}^{n}\frac{(\tau-\tau_i)}{h(-1)^i}\mathscr{F}_1(\xi_i, \eta_i, \zeta_i, \tau_i)d\tau\Big\|_\infty \\
&\leq \frac{\psi}{M(\psi)}\int_{\tau_n}^{\tau_{n+1}} \sum_{i=2}^{n}\prod_{i=2}^{n}\Big|\frac{(\tau-\tau_i)}{h(-1)^i}\Big|\Big\|\mathscr{F}_1(\xi_i, \eta_i, \zeta_i, \tau_i)d\tau\Big\|_\infty \\
&< \frac{\psi}{M(\psi)}\int_{\tau_n}^{\tau_{n+1}} \sum_{i=2}^{n}\prod_{i=2}^{n}\frac{|(\tau-\tau_i)|}{h}i \overset{\sup}{\in} I\Big\{i \overset{\max}{\in} I|\mathscr{F}_1(\xi_i, \eta_i, \zeta_i, \tau_i)|\Big\} \\
&< \frac{\psi}{M(\psi)}\frac{(n+1)!h^{n+1}}{4}M. \\
\|R^n_{2,\psi}\|_\infty &= \frac{\psi}{M(\psi)}\Big\|\int_{\tau_n}^{\tau_{n+1}} \sum_{i=2}^{n}\prod_{i=2}^{n}\frac{(\tau-\tau_i)}{h(-1)^i}\mathscr{F}_2(\xi_i, \eta_i, \zeta_i, \tau_i)d\tau\Big\|_\infty \\
&\leq \frac{\psi}{M(\psi)}\int_{\tau_n}^{\tau_{n+1}} \Big\|\sum_{i=2}^{n}\prod_{i=2}^{n}\frac{(\tau-\tau_i)}{h(-1)^i}\mathscr{F}_2(\xi_i, \eta_i, \zeta_i, \tau_i)d\tau\Big\|_\infty \\
&\leq \frac{\psi}{M(\psi)}\int_{\tau_n}^{\tau_{n+1}} \sum_{i=2}^{n}\prod_{i=2}^{n}\Big|\frac{(\tau-\tau_i)}{h(-1)^i}\Big|\Big\|\mathscr{F}_2(\xi_i, \eta_i, \zeta_i, \tau_i)d\tau\Big\|_\infty \\
&< \frac{\psi}{M(\psi)}\int_{\tau_n}^{\tau_{n+1}} \sum_{i=2}^{n}\prod_{i=2}^{n}\frac{|(\tau-\tau_i)|}{h}i \overset{\sup}{\in} I\Big\{i \overset{\max}{\in} I|\mathscr{F}_2(\xi_i, \eta_i, \zeta_i, \tau_i)|\Big\}
\end{aligned}$$

$$
\begin{aligned}
&< \frac{\psi}{M(\psi)}\frac{(n+1)!h^{n+1}}{4}M.\\
\|R^n_{3,\psi}\|_\infty &= \frac{\psi}{M(\psi)}\left\|\int_{\tau_n}^{\tau_{n+1}}\sum_{i=2}^{n}\prod_{i=2}^{n}\frac{(\tau-\tau_i)}{h(-1)^i}\mathscr{F}_3(\xi_i,\eta_i,\zeta_i,\tau_i)d\tau\right\|_\infty\\
&\leq \frac{\psi}{M(\psi)}\int_{\tau_n}^{\tau_{n+1}}\left\|\sum_{i=2}^{n}\prod_{i=2}^{n}\frac{(\tau-\tau_i)}{h(-1)^i}\mathscr{F}_3(\xi_i,\eta_i,\zeta_i,\tau_i)d\tau\right\|_\infty\\
&\leq \frac{\psi}{M(\psi)}\int_{\tau_n}^{\tau_{n+1}}\sum_{i=2}^{n}\prod_{i=2}^{n}\left|\frac{(\tau-\tau_i)}{h(-1)^i}\right|\left\|\mathscr{F}_3(\xi_i,\eta_i,\zeta_i,\tau_i)d\tau\right\|_\infty\\
&< \frac{\psi}{M(\psi)}\int_{\tau_n}^{\tau_{n+1}}\sum_{i=2}^{n}\prod_{i=2}^{n}\frac{|(\tau-\tau_i)|}{h}i\in I^{\sup}\left\{i\in I^{\max}|\mathscr{F}_3(\xi_i,\eta_i,\zeta_i,\tau_i)|\right\}\\
&< \frac{\psi}{M(\psi)}\frac{(n+1)!h^{n+1}}{4}M.
\end{aligned}
$$

Hence,

$$
\begin{aligned}
\|R^n_{1,\psi}\|_\infty &< \frac{\psi}{M(\psi)}(n+1)!h^{n+1}M.\\
\|R^n_{2,\psi}\|_\infty &< \frac{\psi}{M(\psi)}(n+1)!h^{n+1}M.\\
\|R^n_{3,\psi}\|_\infty &< \frac{\psi}{M(\psi)}(n+1)!h^{n+1}M.
\end{aligned}
$$

Let $\xi(\tau)$, $\eta(\tau)$ and $\zeta(\tau)$ be a solution of ${}^{CF}_{0}D^{\psi}_{t}\xi(\tau) = \mathscr{F}_1(\xi,\eta,\zeta,\tau)$, ${}^{CF}_{0}D^{\psi}_{t}\eta(\tau) = \mathscr{F}_2(\xi,\eta,\zeta,\tau)$, and ${}^{CF}_{0}D^{\psi}_{t}\zeta(\tau) = \mathscr{F}_3(\xi,\eta,\zeta,\tau)$ for every $n \in N$

$$
\begin{aligned}
\|\xi_{n+1}-\xi_n\|_\infty &< \frac{1-\psi}{M(\psi)}\|\mathscr{F}_1(\xi_n,\eta_n,\zeta_n,\tau_n)-\mathscr{F}_1(\xi_{n-1},\eta_{n-1},\zeta_{n-1},\tau_{n-1})\|_\infty\\
&\quad+\frac{\psi h^{n+1}(n+1)!}{4M(\psi)}\\
\|\eta_{n+1}-\eta_n\|_\infty &< \frac{1-\psi}{M(\psi)}\|\mathscr{F}_2(\xi_n,\eta_n,\zeta_n,\tau_n)-\mathscr{F}_2(\xi_{n-1},\eta_{n-1},\zeta_{n-1},\tau_{n-1})\|_\infty\\
&\quad+\frac{\psi h^{n+1}(n+1)!}{4M(\psi)}\\
\|\zeta_{n+1}-\zeta_n\|_\infty &< \frac{1-\psi}{M(\psi)}\|\mathscr{F}_3(\xi_n,\eta_n,\zeta_n,\tau_n)-\mathscr{F}_3(\xi_{n-1},\eta_{n-1},\zeta_{n-1},\tau_{n-1})\|_\infty\\
&\quad+\frac{\psi h^{n+1}(n+1)!}{4M(\psi)}
\end{aligned}
$$

such that if $\|\mathscr{F}_1(\xi_n,\eta_n,\zeta_n,\tau_n)-\mathscr{F}_1(\xi_{n-1},\eta_{n-1},\zeta_{n-1},\tau_{n-1})\|_\infty \to 0$ as $n\to\infty$,

then $\|\xi_{n+1}-\xi_n\|_\infty \to 0$ as $n\to\infty$,

$\|\mathscr{F}_2(\xi_n,\eta_n,\zeta_n,\tau_n)-\mathscr{F}_2(\xi_{n-1},\eta_{n-1},\zeta_{n-1},\tau_{n-1})\|_\infty \to 0$ as $n\to\infty$,

then $\|\eta_{n+1}-\eta_n\|_\infty \to 0$ as $n\to\infty$,

$\|\mathscr{F}_3(\xi_n, \eta_n, \zeta_n, \tau_n) - \mathscr{F}_3(\xi_{n-1}, \eta_{n-1}, \zeta_{n-1}, \tau_{n-1})\|_\infty \to 0$ as $n \to \infty$,
then $\|\zeta_{n+1} - \zeta_n\|_\infty \to 0$ as $n \to \infty$.

Proof.

$$
\begin{aligned}
\|\xi(\tau_{n+1}) - \xi(\tau_n)\| &= \left\| \frac{1-\psi}{M(\psi)} \left[\mathscr{F}_1(\xi_n, \eta_n, \zeta_n, \tau_n) - \mathscr{F}_1(\xi_{n-1}, \eta_{n-1}, \zeta_{n-1}, \tau_{n-1}) \right] \right. \\
&\quad \left. + \frac{\psi}{M(\psi)} \int_{\tau_n}^{\tau_{n+1}} \mathscr{F}_1(\xi, \eta, \zeta, \tau) d\tau \right\|_\infty \\
&\leq \frac{1-\psi}{M(\psi)} \|\mathscr{F}_1(\xi_n, \eta_n, \zeta_n, \tau_n) - \mathscr{F}_1(\xi_{n-1}, \eta_{n-1}, \zeta_{n-1}, \tau_{n-1})\| \\
&\quad + \frac{\psi}{M(\psi)} \left\| \int_{\tau_n}^{\tau_{n+1}} \mathscr{F}_1(\xi, \eta, \zeta, \tau) d\tau \right\|_\infty \\
&\leq \frac{1-\psi}{M(\psi)} \|\mathscr{F}_1(\xi_n, \eta_n, \zeta_n, \tau_n) - \mathscr{F}_1(\xi_{n-1}, \eta_{n-1}, \zeta_{n-1}, \tau_{n-1})\| \\
&\quad + \frac{\psi}{M(\psi)} \int_{\tau_n}^{\tau_{n+1}} \left| \sum_{i=0}^{n} \prod_{i=0}^{n} \frac{(\tau - \tau_i)}{h(-1)} \right|_\infty d\tau \\
&< \frac{1-\psi}{M(\psi)} \|\mathscr{F}_2(\xi_n, \eta_n, \zeta_n, \tau_n) - \mathscr{F}_2(\xi_{n-1}, \eta_{n-1}, \zeta_{n-1}, \tau_{n-1})\|_\infty + \frac{\psi h^{n+1}(n+1)!}{4M(\psi)} \\
\|\eta(\tau_{n+1}) - \eta(\tau_n)\| &= \left\| \frac{1-\psi}{M(\psi)} \left[\mathscr{F}_2(\xi_n, \eta_n, \zeta_n, \tau_n) - \mathscr{F}_2(\xi_{n-1}, \eta_{n-1}, \zeta_{n-1}, \tau_{n-1}) \right] \right. \\
&\quad \left. + \frac{\psi}{M(\psi)} \int_{\tau_n}^{\tau_{n+1}} \mathscr{F}_2(\xi, \eta, \zeta, \tau) d\tau \right\|_\infty \\
&\leq \frac{1-\psi}{M(\psi)} \|\mathscr{F}_2(\xi_n, \eta_n, \zeta_n, \tau_n) - \mathscr{F}_2(\xi_{n-1}, \eta_{n-1}, \zeta_{n-1}, \tau_{n-1})\| \\
&\quad + \frac{\psi}{M(\psi)} \left\| \int_{\tau_n}^{\tau_{n+1}} \mathscr{F}_2(\xi, \eta, \zeta, \tau) d\tau \right\|_\infty \\
&\leq \frac{1-\psi}{M(\psi)} \|\mathscr{F}_2(\xi_n, \eta_n, \zeta_n, \tau_n) - \mathscr{F}_2(\xi_{n-1}, \eta_{n-1}, \zeta_{n-1}, \tau_{n-1})\| \\
&\quad + \frac{\psi}{M(\psi)} \int_{\tau_n}^{\tau_{n+1}} \left| \sum_{i=0}^{n} \prod_{i=0}^{n} \frac{(\tau - \tau_i)}{h(-1)} \right|_\infty d\tau \qquad (6.7) \\
&< \frac{1-\psi}{M(\psi)} \|\mathscr{F}_2(\xi_n, \eta_n, \zeta_n, \tau_n) - \mathscr{F}_2(\xi_{n-1}, \eta_{n-1}, \zeta_{n-1}, \tau_{n-1})\|_\infty + \frac{\psi h^{n+1}(n+1)!}{4M(\psi)} \\
\|\zeta(\tau_{n+1}) - \zeta(\tau_n)\| &= \left\| \frac{1-\psi}{M(\psi)} \left[\mathscr{F}_3(\xi_n, \eta_n, \zeta_n, \tau_n) - \mathscr{F}_3(\xi_{n-1}, \eta_{n-1}, \zeta_{n-1}, \tau_{n-1}) \right] \right. \\
&\quad \left. + \frac{\psi}{M(\psi)} \int_{\tau_n}^{\tau_{n+1}} \mathscr{F}_3(\xi, \eta, \zeta, \tau) d\tau \right\|_\infty \\
&\leq \frac{1-\psi}{M(\psi)} \|\mathscr{F}_3(\xi_n, \eta_n, \zeta_n, \tau_n) - \mathscr{F}_3(\xi_{n-1}, \eta_{n-1}, \zeta_{n-1}, \tau_{n-1})\|
\end{aligned}
$$

$$
\begin{aligned}
&+ \frac{\psi}{M(\psi)} \left\| \int_{\tau_n}^{\tau_{n+1}} \mathscr{F}_3(\xi, \eta, \zeta, \tau) d\tau \right\|_\infty \\
&\leq \frac{1-\psi}{M(\psi)} \|\mathscr{F}_3(\xi_n, \eta_n, \zeta_n, \tau_n) - \mathscr{F}_3(\xi_{n-1}, \eta_{n-1}, \zeta_{n-1}, \tau_{n-1})\| \\
&+ \frac{\psi}{M(\psi)} \int_{\tau_n}^{\tau_{n+1}} \left| \sum_{i=0}^{n} \prod_{i=0}^{n} \frac{(\tau - \tau_i)}{h(-1)} \right|_\infty d\tau \\
&< \frac{1-\psi}{M(\psi)} \|\mathscr{F}_3(\xi_n, \eta_n, \zeta_n, \tau_n) - \mathscr{F}_3(\xi_{n-1}, \eta_{n-1}, \zeta_{n-1}, \tau_{n-1})\|_\infty + \frac{\psi h^{n+1}(n+1)!}{4M(\psi)}
\end{aligned}
$$

$$
\begin{aligned}
&\text{So if } \|\mathscr{F}_1(\xi_n, \eta_n, \zeta_n, \tau_n) - \mathscr{F}_1(\xi_{n-1}, \eta_{n-1}, \zeta_{n-1}, \tau_{n-1})\|_\infty \to 0 \text{ as } n \to \infty, \\
&\quad \text{then } \|\xi_{n+1} - \xi_n\|_\infty \to 0 \text{ as } n \to \infty, \\
&\quad \|\mathscr{F}_2(\xi_n, \eta_n, \zeta_n, \tau_n) - \mathscr{F}_2(\xi_{n-1}, \eta_{n-1}, \zeta_{n-1}, \tau_{n-1})\|_\infty \to 0 \text{ as } n \to \infty, \\
&\quad \text{then } \|\eta_{n+1} - \eta_n\|_\infty \to 0 \text{ as } n \to \infty, \\
&\quad \|\mathscr{F}_3(\xi_n, \eta_n, \zeta_n, \tau_n) - \mathscr{F}_3(\xi_{n-1}, \eta_{n-1}, \zeta_{n-1}, \tau_{n-1})\|_\infty \to 0 \text{ as } n \to \infty, \\
&\quad \text{then } \|\zeta_{n+1} - \zeta_n\|_\infty \to 0 \text{ as } n \to \infty.
\end{aligned}
$$

From the analysis, we have shown that the proposed numerical scheme satisfies the necessary conditions for stability and convergence. By ensuring the boundedness of $R^n_{1,\psi}$, $R^n_{2,\psi}$ and $R^n_{3,\psi}$ ensure stability. The method's second-order convergence and compatibility with non-singular fractional operators make it a suitable approach for simulating chaotic systems with memory effects governed by Caputo-Fabrizio derivatives.

7. Numerical simulation

In this section, we implement the numerical scheme from Section 5 to generate graphical representations of the multi-bond orbital chaotic attractor governed by the Caputo–Fabrizio fractional derivative. All simulations are carried out using a fixed step size of $h = 0.01$. The parameter values used in this study (r, s, C, P, and Q) are selected based on the work of Zhang et al. [41], who demonstrated that these configurations produce multi-bond orbital chaotic attractors with rich dynamical characteristics, including sustained chaotic oscillations and multiscroll topologies.

7.1. The classical case, when $\psi = 1$.

In this section, we consider the classical case, that is, when $\psi = 1$. When we substitute $\psi = 1$ in (5.7), we obtain the following systems of equations:

$$
\begin{aligned}
\xi_{n+1} &= \xi_n + \frac{3h}{2}\mathscr{F}_1(\xi_n, \eta_n, \zeta_n, \tau_n) + \frac{h}{2}\mathscr{F}_1(\xi_{n-1}, \eta_{n-1}, \zeta_{n-1}, \tau_{n-1}) \\
\eta_{n+1} &= \eta_n + \frac{3h}{2}\mathscr{F}_2(\xi_n, \eta_n, \zeta_n, \tau_n) + \frac{h}{2}\mathscr{F}_2(\xi_{n-1}, \eta_{n-1}, \zeta_{n-1}, \tau_{n-1}) \\
\zeta_{n+1} &= \zeta_n + \frac{3h}{2}\mathscr{F}_3(\xi_n, \eta_n, \zeta_n, \tau_n) + \frac{h}{2}\mathscr{F}_3(\xi_{n-1}, \eta_{n-1}, \zeta_{n-1}, \tau_{n-1})
\end{aligned} \tag{7.1}
$$

Substituting the same value of $\psi = 1$ into Eq (4.1) yields the integer order derivative, which brings us back to the equation in (3.1). Using Eq (7.1), different parameter values, and initial conditions, we obtain the following graphical simulations.

7.2. The fractional case when $0 < \psi < 1$

In this section, we consider the fractional case when $\psi \neq 1$. This means we use the following system of equations to obtain our graphical simulations for different values of ψ. Hence, we use the systems of equations in (5.7) defined as follows:

$$\begin{aligned}
\xi_{n+1} &= \xi_n + \Big(\frac{1-\psi}{M(\psi)} + \frac{3\psi h}{2M(\psi)}\Big)\mathscr{F}_1(\xi_n, \eta_n, \zeta_n, \tau_n) \\
&\quad + \Big(\frac{1-\psi}{M(\psi)} + \frac{\psi h}{2M(\psi)}\Big)\mathscr{F}_1(\xi_{n-1}, \eta_{n-1}, \zeta_{n-1}, \tau_{n-1}) \\
\eta_{n+1} &= \eta_n + \Big(\frac{1-\psi}{M(\psi)} + \frac{3\psi h}{2M(\psi)}\Big)\mathscr{F}_2(\xi_n, \eta_n, \zeta_n, \tau_n) \\
&\quad + \Big(\frac{1-\psi}{M(\psi)} + \frac{\psi h}{2M(\psi)}\Big)\mathscr{F}_2(\xi_{n-1}, \eta_{n-1}, \zeta_{n-1}, \tau_{n-1}) \\
\zeta_{n+1} &= \zeta_n + \Big(\frac{1-\psi}{M(\psi)} + \frac{3\psi h}{2M(\psi)}\Big)\mathscr{F}_3(\xi_n, \eta_n, \zeta_n, \tau_n) \\
&\quad + \Big(\frac{1-\psi}{M(\psi)} + \frac{\psi h}{2M(\psi)}\Big)\mathscr{F}_3(\xi_{n-1}, \eta_{n-1}, \zeta_{n-1}, \tau_{n-1})
\end{aligned}$$

Bifurcation analysis

To explore the nonlinear behavior of the fractional-order MBOCA system, we perform a bifurcation analysis by varying the system parameter r while keeping other parameters fixed.

8. Discussion

In this work, we have analyzed the multi-bond orbital chaotic attractor (MBOCA) under both integer order and fractional order formulations. For the fractional case, the Caputo-Fabrizio fractional operator is adopted to solve the system. To recover the classical integer order case, we set $\psi = 1$, producing the graphical results presented in Figures 1–8. For the fractional order case, where $0 < \psi < 1$, the corresponding results are depicted in Figures 9–14, using various parameter configurations.

In the integer order scenario ($\psi = 1$), we observe that different phase portraits emerge as system parameters vary. For example, with initial conditions $[\xi(0), \eta(0), \zeta(0)] = [2.972, 0.1, 0]$ and parameter values $r = -1.45$, $s = 1.45$, $C = 0.7$, and $P = Q = 4$, the phase portrait exhibits a twofold scroll structure (see Figure 2). When changing to initial conditions $[1.5, 0.9, 0]$ while maintaining $r = -1.45$, $s = 1.45$, $C = 0.6$, and $P = Q = 4$, a threefold structure is obtained, as shown in Figure 4.

Furthermore, Figure 6 demonstrates a fourfold attractor, which is obtained using the same parameters as Figure 4 but with initial conditions $[0.1, 0.8, 0]$. These results highlight that both C and the initial conditions strongly influence the number of scrolls generated. When the sign of r is changed, the results depicted in Figures 7 and 8 emerge. Notably, Figure 8 reveals a nine-scroll structure. These multiple scroll structures are more distinctly observable in the ξ–η, ξ–ζ, and ξ–η–ζ

projections, compared to the η–ζ plane. Collectively, these findings confirm that the structure of the MBOCA is highly sensitive to coupling parameter C and the initial conditions, with the number of scrolls increasing as these parameters vary.

In the fractional order case ($0 < \psi < 1$), the system exhibits phase portraits qualitatively distinct from their integer order counterparts. From Figures 9–14, it is evident that varying ψ enables the generation of attractors with different scroll patterns, even under identical initial conditions $[1.5, 0.9, 0]$. These observations suggest that fractional calculus provides an enhanced modeling framework for chaotic systems, introducing greater flexibility and tunability through the fractional order parameter ψ. To further investigate the system's nonlinear dynamics under the fractional-order framework, a bifurcation analysis is performed by varying the system parameter r, as shown in Figure 15. The bifurcation diagram reveals distinct transitions from periodic to chaotic behavior as r increases, demonstrating the system's sensitivity to this parameter. These results complement the phase portraits and confirm that not only the initial conditions and fractional order ψ, but also specific system parameters such as r, significantly influence the qualitative behavior of the MBOCA system.

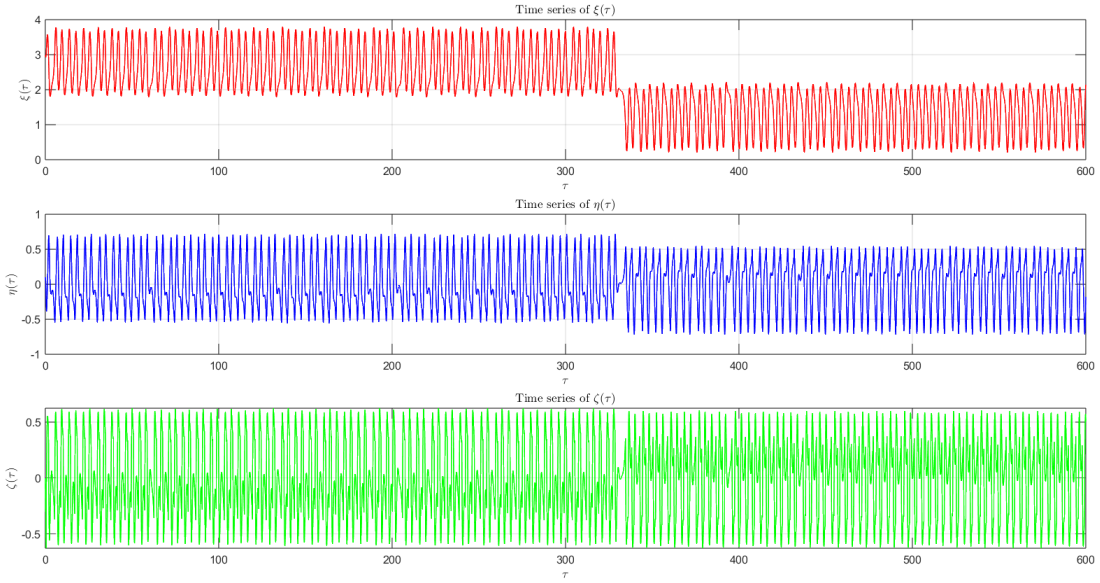

Figure 1. Time series of the MBOCA system variables with initial condition $[2.972, 0.1, 0]$ and parameters $r = -1.45$, $s = 1.45$, $C = 0.70$, $P = Q = 4$, and $\psi = 1$. The plots show the evolution of (top) $\xi(\tau)$, (middle) $\eta(\tau)$, and (bottom) $\zeta(\tau)$ over the time interval $[0, 600]$.

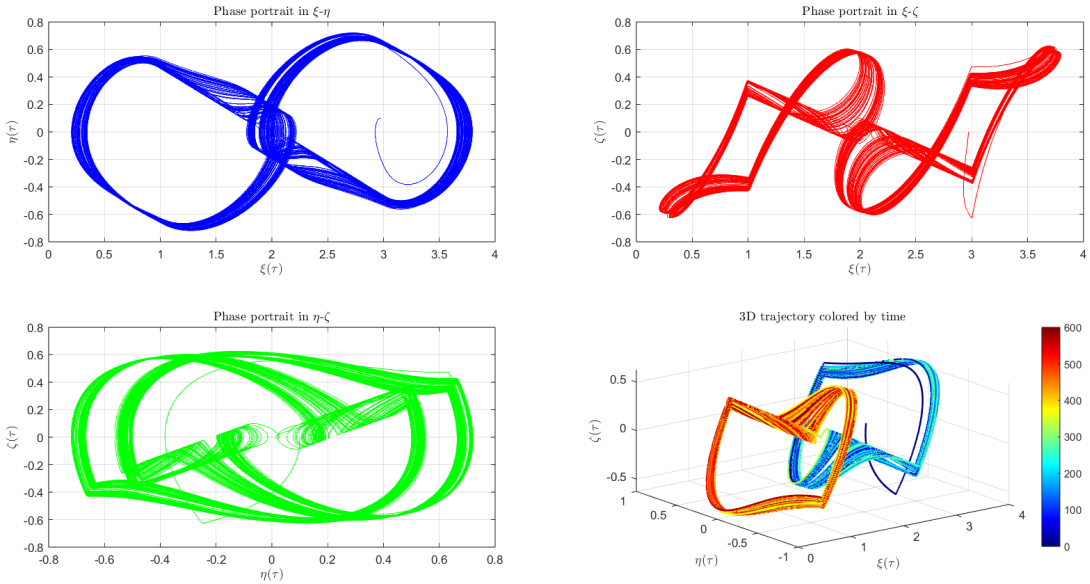

Figure 2. Phase portraits of the MBOCA system exhibiting a twofold chaotic structure, generated using parameters $r = -1.45$, $s = 1.45$, $C = 0.70$, $P = Q = 4$, and $\psi = 1$, with initial condition [2.972, 0.1, 0]. The figure shows 2D projections in the (ξ, η), (ξ, ζ), and (η, ζ) planes, along with the 3D trajectory colored by simulation time.

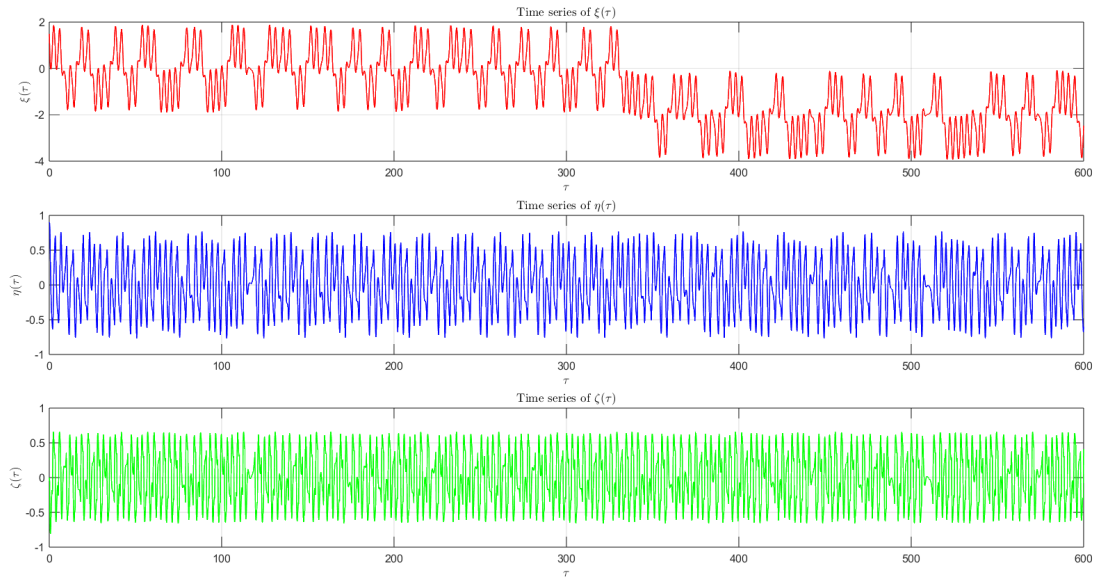

Figure 3. Time series of the MBOCA system variables with initial condition [1.5, 0.9, 0] and parameters $r = -1.45$, $s = 1.45$, $C = 0.60$, $P = Q = 4$, and $\psi = 1$. The plots show the evolution of (top) $\xi(\tau)$, (middle) $\eta(\tau)$, and (bottom) $\zeta(\tau)$ over the time interval $[0, 600]$.

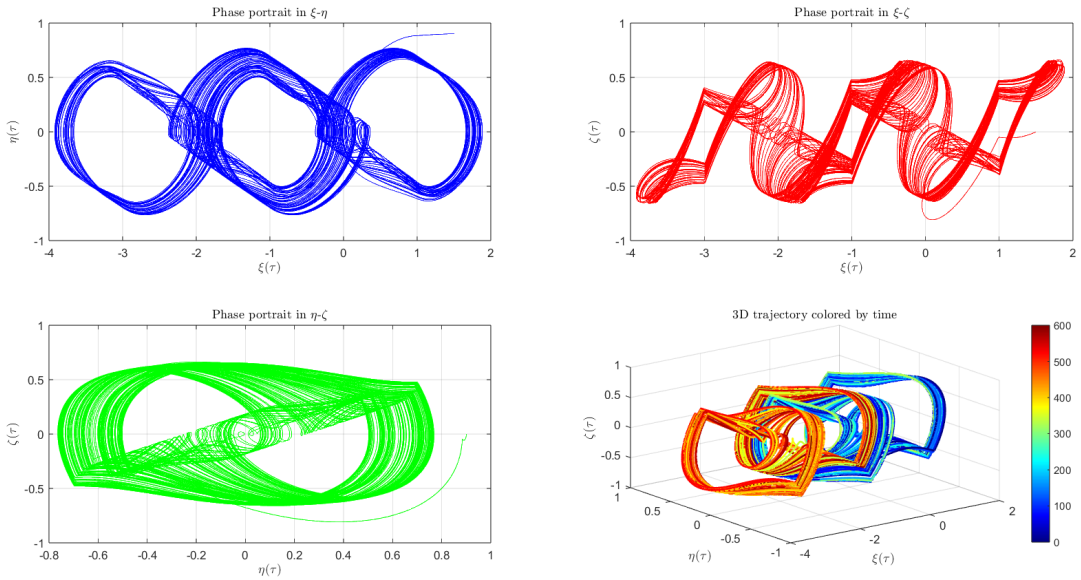

Figure 4. Phase portraits of the MBOCA system exhibiting a threefold chaotic structure, generated using parameters $r = -1.45$, $s = 1.45$, $C = 0.60$, $P = Q = 4$, and $\psi = 1$, with initial condition [1.5, 0.9, 0]. The figure shows 2D projections in the (ξ, η), (ξ, ζ), and (η, ζ) planes, along with the 3D trajectory colored by simulation time.

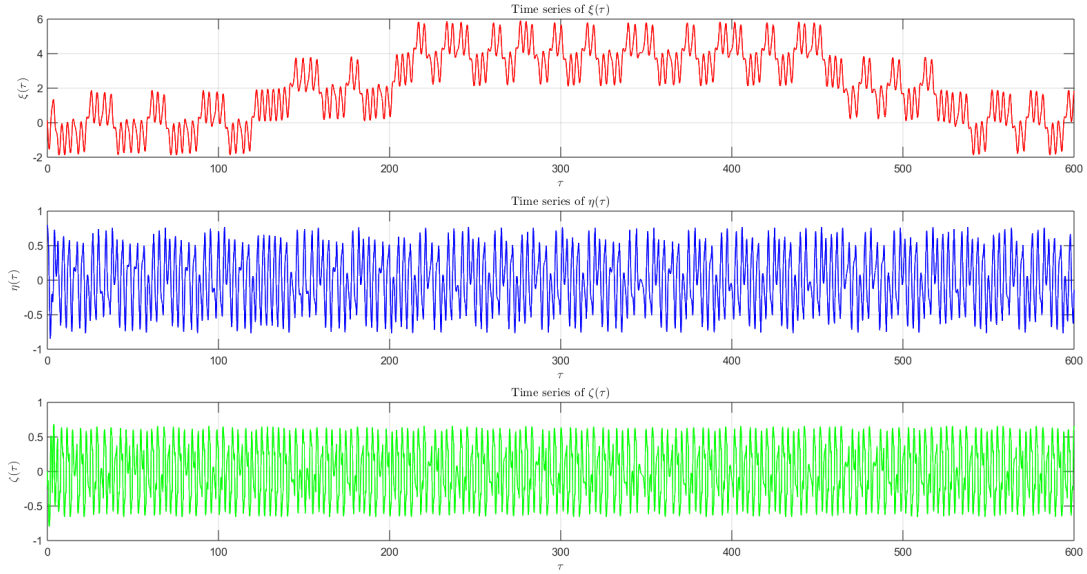

Figure 5. Time series of the MBOCA system variables with initial condition [1.1, 0.8, 0] and parameters $r = -1.45$, $s = 1.45$, $C = 0.60$, $P = Q = 4$, and $\psi = 1$. The plots show the evolution of (top) $\xi(\tau)$, (middle) $\eta(\tau)$, and (bottom) $\zeta(\tau)$ over the time interval $[0, 600]$.

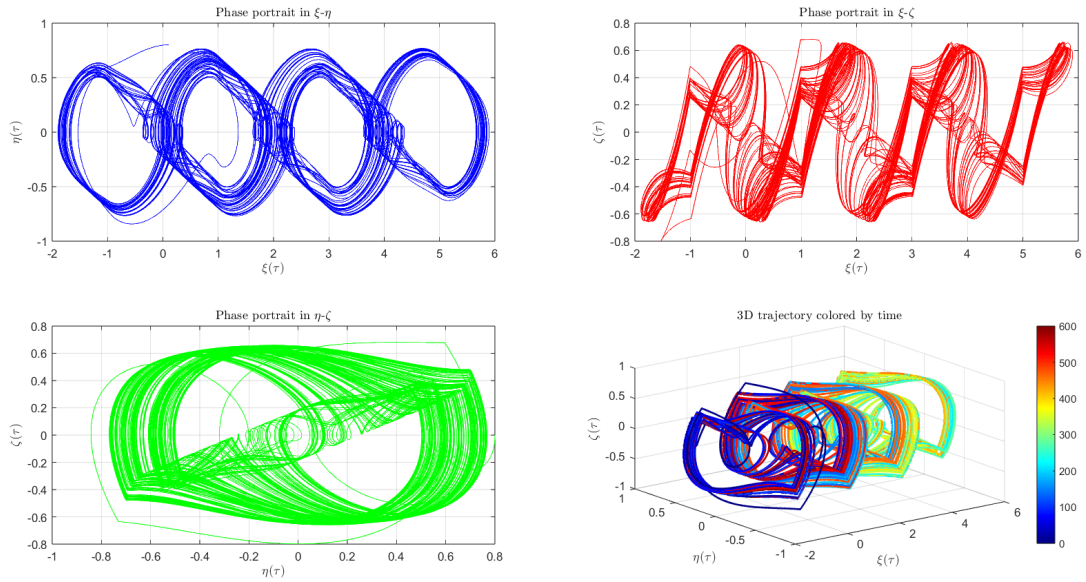

Figure 6. Phase portraits of the MBOCA system exhibiting a fourfold chaotic structure, generated using parameters $r = -1.45$, $s = 1.45$, $C = 0.60$, $P = Q = 4$, and $\psi = 1$, with initial condition [0.1, 0.8, 0]. The figure shows 2D projections in the (ξ, η), (ξ, ζ), and (η, ζ) planes, along with the 3D trajectory colored by simulation time.

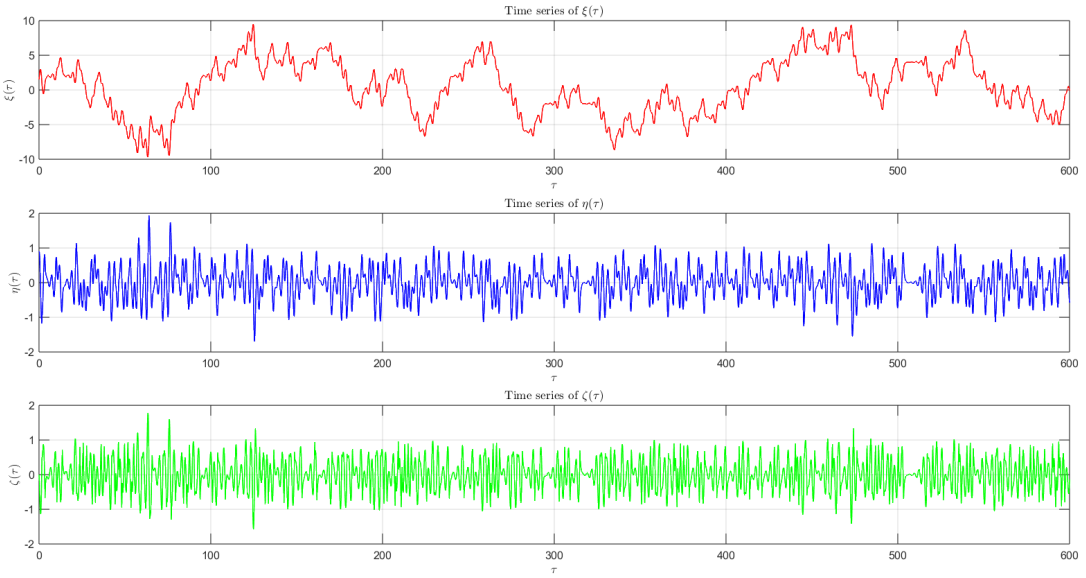

Figure 7. Time series of the MBOCA system variables with initial condition [1.5, 0.9, 0] and parameters $r = 1.45$, $s = 1.45$, $C = 0.60$, $P = Q = 4$, and $\psi = 1$. The plots show the evolution of (top) $\xi(\tau)$, (middle) $\eta(\tau)$, and (bottom) $\zeta(\tau)$ over the time interval $[0, 600]$.

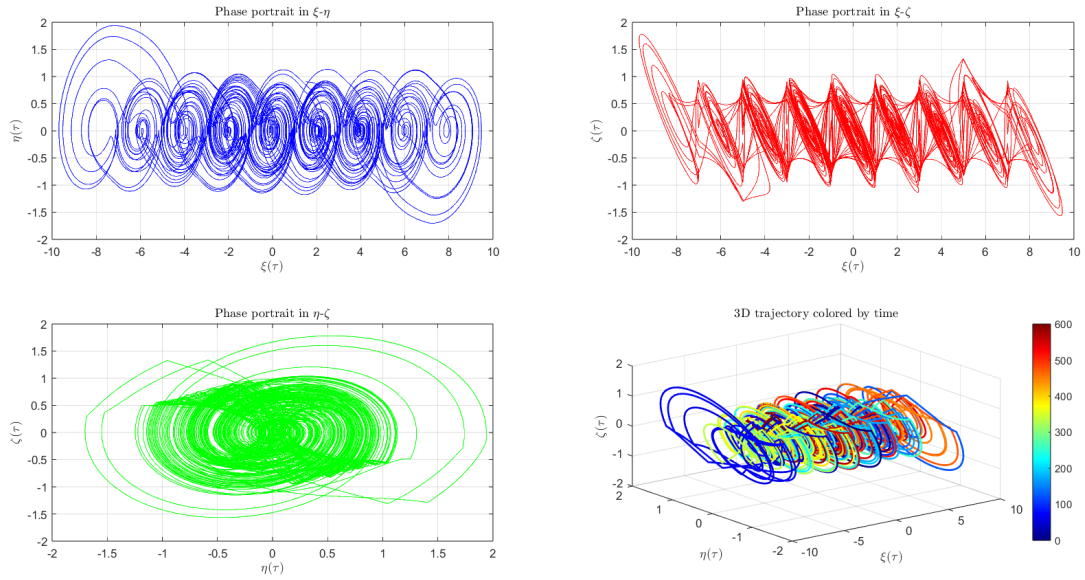

Figure 8. Phase portraits of the MBOCA system, generated using parameters $r = 1.45$, $s = 1.45$, $C = 0.60$, $P = Q = 4$, and $\psi = 1$, with initial condition [1.5, 0.9, 0]. The figure shows 2D projections in the (ξ, η), (ξ, ζ), and (η, ζ) planes, along with the 3D trajectory colored by simulation time.

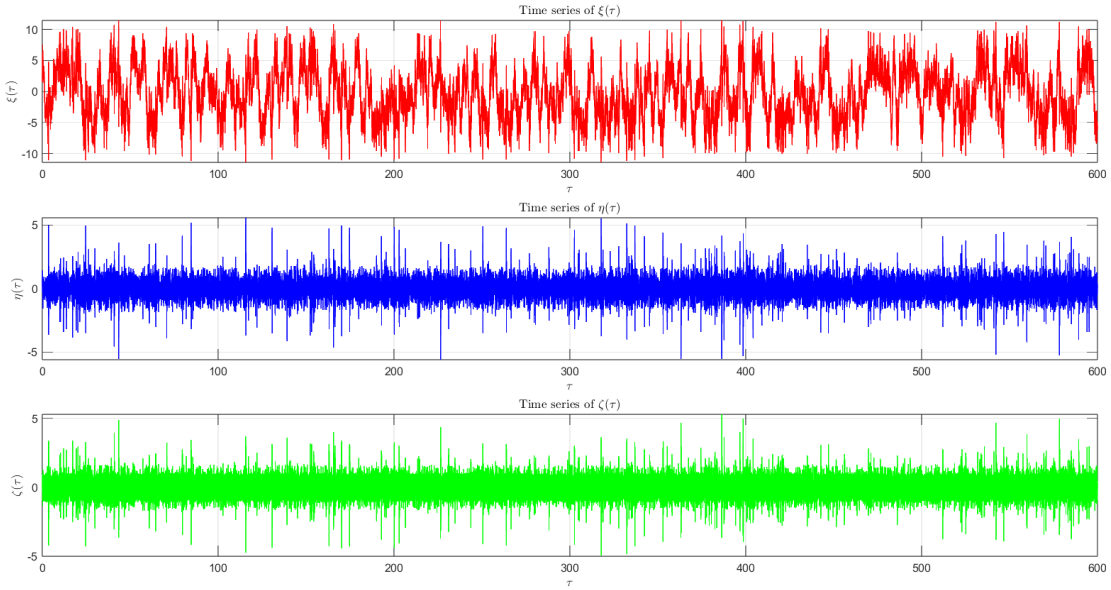

Figure 9. Time series of the MBOCA system variables with initial condition [1.5, 0.9, 0] and parameters $r = 1.45$, $s = 1.45$, $C = 0.70$, $P = Q = 4$, and $\psi = 0.89$. The plots show the evolution of (top) $\xi(\tau)$, (middle) $\eta(\tau)$, and (bottom) $\zeta(\tau)$ over the time interval $[0, 600]$.

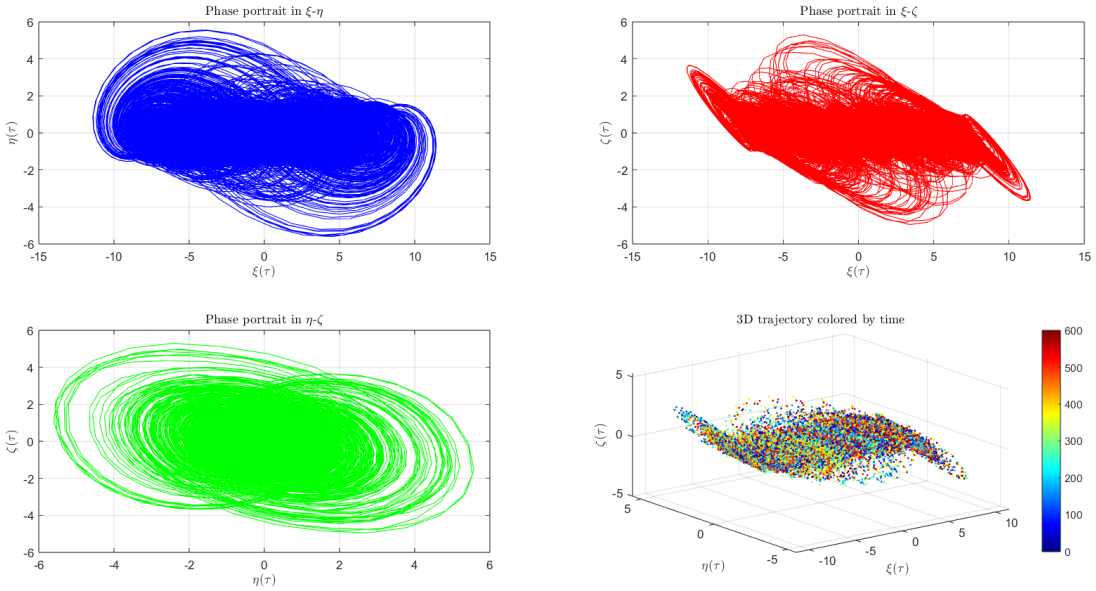

Figure 10. Phase portraits of the MBOCA system, generated using parameters $r = 1.45$, $s = 1.45$, $C = 0.70$, $P = Q = 4$, and $\psi = 0.89$, with initial condition [1.5, 0.9, 0]. The figure shows 2D projections in the (ξ, η), (ξ, ζ), and (η, ζ) planes, along with the 3D trajectory colored by simulation time.

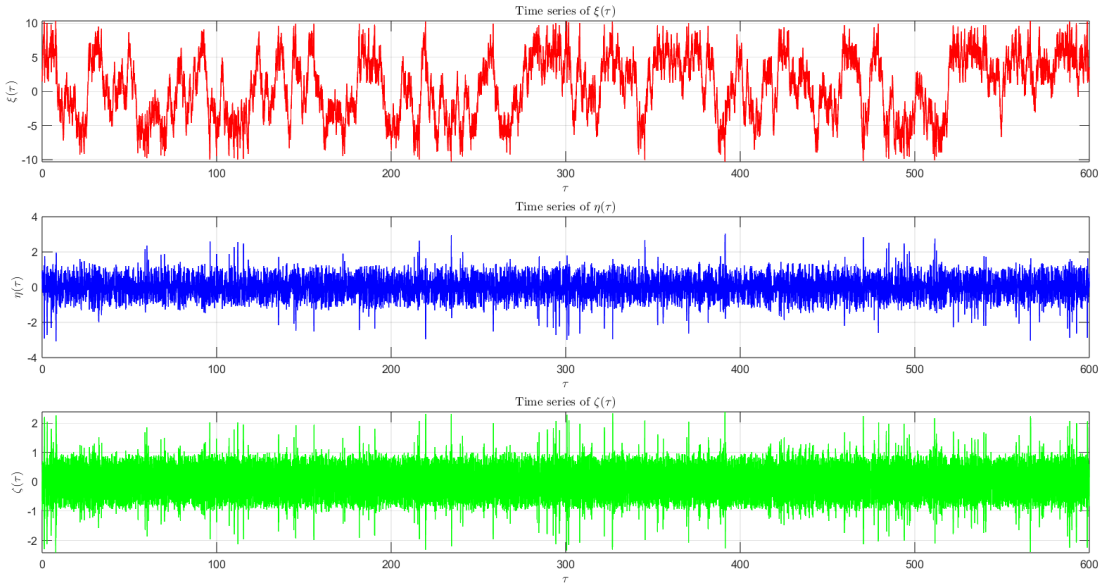

Figure 11. Time series of the MBOCA system variables with initial condition [1.5, 0.9, 0] and parameters $r = 1.45$, $s = 1.45$, $C = 0.70$, $P = Q = 4$, and $\psi = 0.95$. The plots show the evolution of (top) $\xi(\tau)$, (middle) $\eta(\tau)$, and (bottom) $\zeta(\tau)$ over the time interval $[0, 600]$.

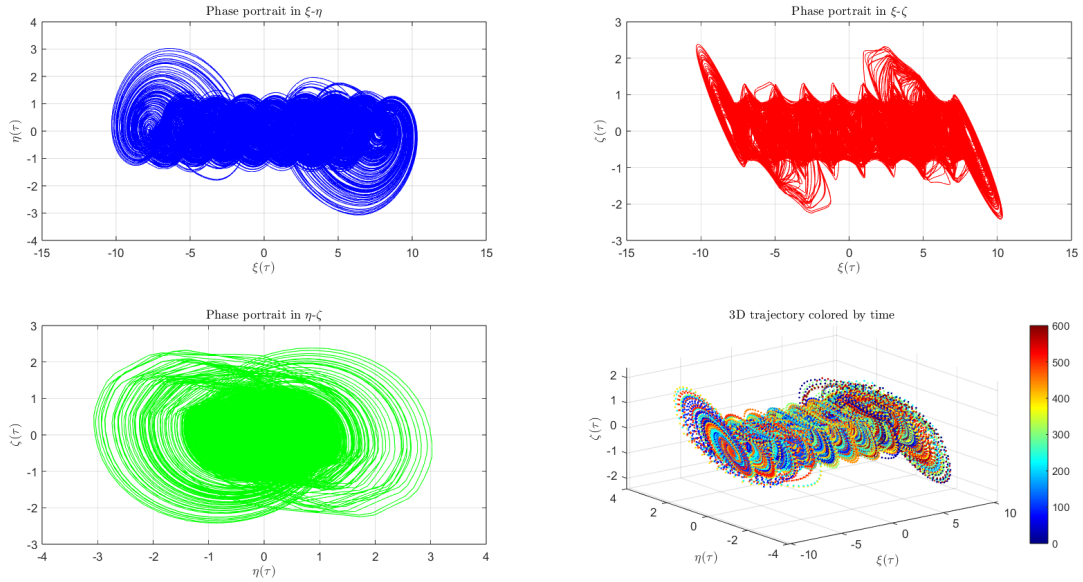

Figure 12. Phase portraits of the MBOCA system, generated using parameters $r = 1.45$, $s = 1.45$, $C = 0.70$, $P = Q = 4$, and $\psi = 0.95$, with initial condition [1.5, 0.9, 0]. The figure shows 2D projections in the (ξ, η), (ξ, ζ), and (η, ζ) planes, along with the 3D trajectory colored by simulation time.

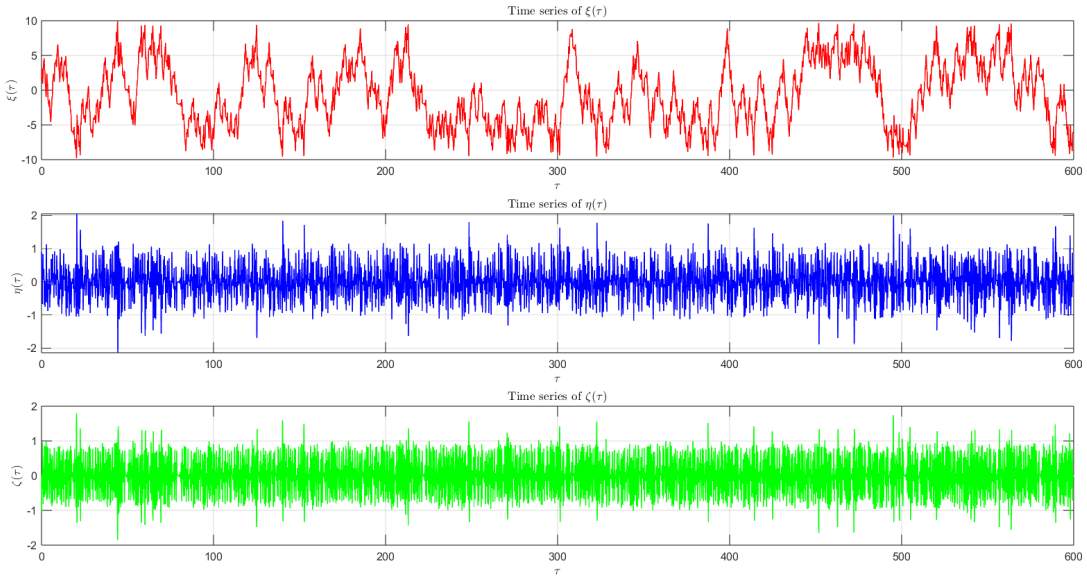

Figure 13. Time series of the MBOCA system variables with initial condition [1.5, 0.9, 0] and parameters $r = 1.45$, $s = 1.45$, $C = 0.70$, $P = Q = 4$, and $\psi = 0.98$. The plots show the evolution of (top) $\xi(\tau)$, (middle) $\eta(\tau)$, and (bottom) $\zeta(\tau)$ over the time interval $[0, 600]$.

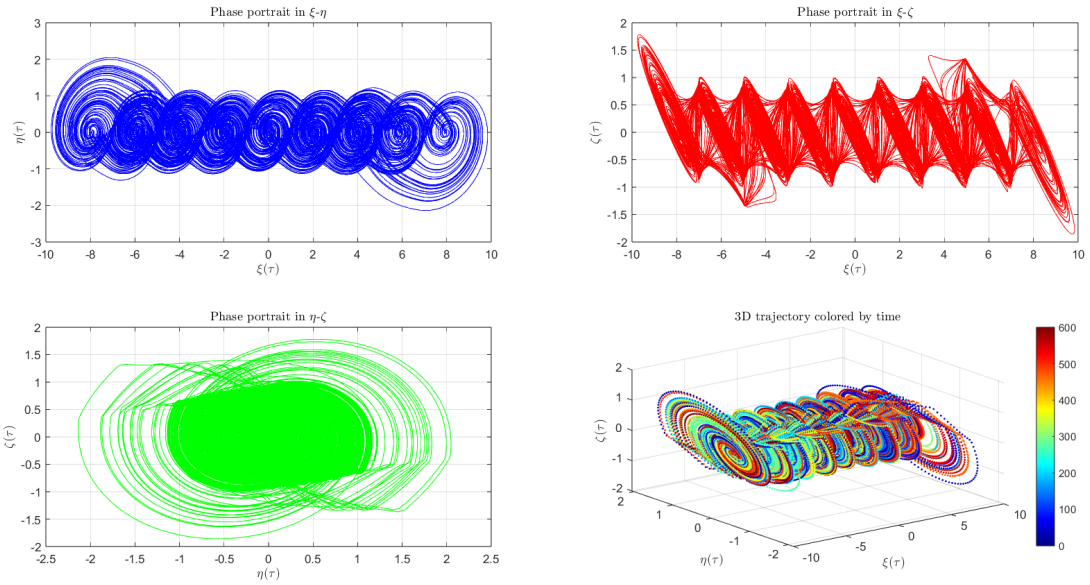

Figure 14. Phase portraits of the MBOCA system, generated using parameters $r = 1.45$, $s = 1.45$, $C = 0.70$, $P = Q = 4$, and $\psi = 0.98$, with initial condition [1.5, 0.9, 0]. The figure shows 2D projections in the (ξ, η), (ξ, ζ), and (η, ζ) planes, along with the 3D trajectory colored by simulation time.

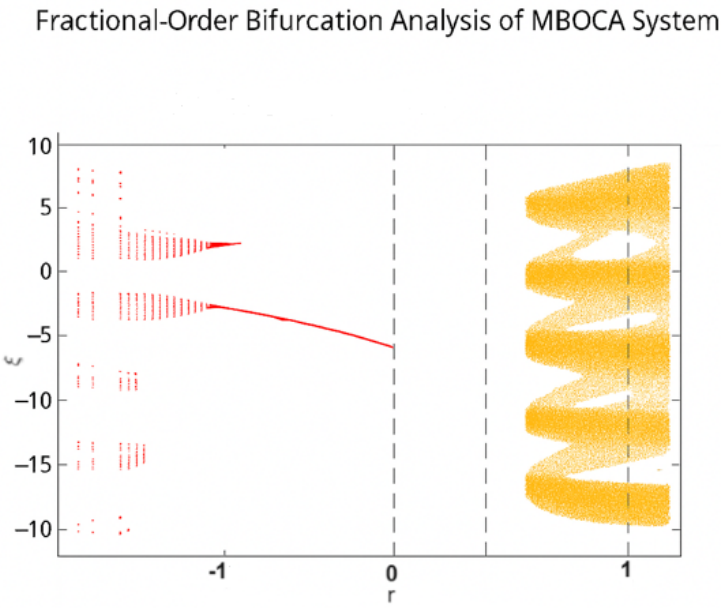

Figure 15. Bifurcation diagram of the MBOCA system with respect to parameter r, generated using the Caputo-Fabrizio fractional derivative with order $\psi = 0.98$. The system is simulated with fixed parameters $s = 1.45$, $C = 0.70$, and $P = Q = 4$, and initial condition [1.5, 0.9, 0]. The plot shows the long-term values of the state variable ξ, revealing transitions from periodic to chaotic behavior as r increases.

9. Conclusions

In this paper, we have investigated the multi-bond orbital chaotic attractor (MBOCA) by extending its classical integer-order formulation to a fractional-order model using the Caputo-Fabrizio fractional derivative. We established existence and uniqueness results for the fractional-order system, derived a suitable numerical scheme, and analyzed its convergence and stability. Numerical simulations confirmed that the fractional-order parameter introduces significant flexibility and enriches the dynamic behavior of the system. In particular, the results demonstrated how varying the fractional-order parameter ψ can produce qualitatively distinct chaotic attractors compared to the integer-order case, highlighting the sensitivity of the system to initial conditions and control parameters. Furthermore, bifurcation analysis revealed how changes in ψ influence the transition between dynamical regimes, including periodic and chaotic states. This reinforces the role of fractional-order parameters as effective tools for modulating system complexity. These findings suggest that fractional operators, especially those with non-singular kernels like Caputo-Fabrizio, offer powerful tools for enhancing the modeling and analysis of complex chaotic systems. Future research may entail the application of other fractional operators, parameter identification techniques, and control strategies to further understand and leverage the complex behavior of MBOCA systems for engineering and secure communication applications.

Author contributions

All authors contributed to the conception, methodology, analysis, and writing of this manuscript. All authors reviewed and approved the final version.

Use of Generative-AI tools declaration

The authors declare they have not used Artificial Intelligence (AI) tools in the creation of this article.

Acknowledgments

We thank all colleagues and mentors who contributed to this study. This work was supported by the University of South Africa (UNISA). We also appreciate the reviewers and editorial team for their valuable feedback.

Conflict of interest

The authors declare that they have no conflicts of interest.

References

1. M. Abu-Shady, M. K. A. Kaabar, A generalized definition of the fractional derivative with applications, *Math. Probl. Eng.,* **2021** (2021), 1–9. https://doi.org/10.1155/2021/9444803

2. K. Diethelm, V. Kiryakova, Y. Luchko, J. A. T. Machado, V. E. Tarasov, Trends, directions for further research, and some open problems of fractional calculus, *Nonlinear Dyn.,* **107** (2022), 3245–3270. https://doi.org/10.1007/s11071-021-07158-9

3. G. Huang, H. Y. Qin, Q. Chen, Z. Shi, S. Jiang, C. Huang, Research on application of fractional calculus operator in image underlying processing, *Fractal Fract.,* **8** (2024), 37. https://doi.org/10.3390/fractalfract8010037

4. E. Viera-Martin, J. F. Gómez-Aguilar, J. E. Solís-Pérez, J. A. Hernández-Pérez, R. F. Escobar-Jiménez, Artificial neural networks: A practical review of applications involving fractional calculus, *Eur. Phys. J.-Spec. Top.,* **231** (2022), 2059–2095. https://doi.org/10.1140/epjs/s11734-022-00455-3

5. L. C. de Barros, M. M. Lopes, F. S. Pedro, E. Esmi, J. P. C. dos Santos, D. E. Sánchez, The memory effect on fractional calculus: An application in the spread of COVID-19, *Comput. Appl. Math.,* **40** (2021), 1–21. https://doi.org/10.1007/s40314-021-01456-z

6. R. E. Gutierrez, J. M. Rosario, J. A. T. Machado, Fractional order calculus: basic concepts and engineering applications, *Math. Probl. Eng.,* **2010** (2010). https://doi.org/10.1155/2010/375858

7. M. I. Syam, M. Al-Refai, Fractional differential equations with Atangana–Baleanu fractional derivative: Analysis and applications, *Chaos Soliton. Fract.,* **2** (2019), 100013. https://doi.org/10.1016/S2590-1486(19)30013-5

8. A. Ali, S. Das, Applications of neuro-computing and fractional calculus to blood streaming conveying modified trihybrid nanoparticles with interfacial nanolayer aspect inside a diseased ciliated artery under electroosmotic and Lorentz forces, *Int. Commun. Heat Mass,* **152** (2024), 107313. https://doi.org/10.1016/j.icheatmasstransfer.2024.107313

9. T. Alinei-Poiana, E. H. Dulf, L. Kovacs, Fractional calculus in mathematical oncology, *Sci. Rep.,* **13** (2023), 10083. https://doi.org/10.1038/s41598-023-37196-9

10. C. Da Silva, M. Peces, A. Jaques, J. J. Muñoz, J. Dosta, S. Astals, Fractional calculus as a generalized kinetic model for biochemical methane potential tests, *Bioresource Technol.,* **396** (2024), 130412. https://doi.org/10.1016/j.biortech.2024.130412

11. M. A. Hernández-Pérez, G. Delgado-Reyes, V. Borja-Jaimes, J. S. Valdez-Martínez, M. Cervantes-Bobadilla, An adaptation of a sliding mode classical observer to a fractional-order observer for disturbance reconstruction of a UAV model: A Riemann–Liouville fractional calculus approach, *Mathematics,* **11** (2023), 4876. https://doi.org/10.3390/math11244876

12. H. Pratap, S. Kumar, G. Singh, Brief history of fractional calculus: A survey, *Migr. Lett.,* **21** (2024), 238–243.

13. R. Hilfer, Fractional diffusion based on Riemann-Liouville fractional derivatives, *J. Phys. Chem. B,* **104** (2000), 3914–3917. https://doi.org/10.1021/jp9936289

14. A. Atangana, K. M. Owolabi, New numerical approach for fractional differential equations, *Math. Model. Nat. Pheno.,* **13** (2018), 3. Available from: `https://www.mmnp-journal.org/10.1051/mmnp/2021039`.

15. A. Atangana, D. Baleanu, *New fractional derivatives with nonlocal and non-singular kernel: Theory and application to heat transfer model*, *arXiv preprint,* 2016. https://doi.org/10.48550/arXiv.1602.03408

16. R. B. Albadarneh, I. M. Batiha, A. Adwai, N. Tahat, A. K. Alomari, Numerical approach of Riemann-Liouville fractional derivative operator, *Int. J. Electr. Comput. Eng.,* **11** (2021), 5367–5378. https://doi.org/10.11591/IJECE.V11I6.PP5367-5378

17. G. Farid, Bounds of Riemann-Liouville fractional integral operators, *Comput. Methods Diffe.,* **9** (2021), 637–648. https://doi.org/10.22034/cmde.2020.32653.1516

18. M. Caputo, M. Fabrizio, A new definition of fractional derivative without singular kernel, *Prog. Fract. Diff. Appl.,* **1** (2015), 73–85. http://dx.doi.org/10.12785/pfda/010201

19. A. Atangana, Application of fractional calculus to epidemiology, *Fract. Dyn.,* 2015, 174–190.

20. I. Ahmed, E. F. D. Goufo, A. Yusuf, P. Kumam, P. Chaipanya, K. Nonlaopon, An epidemic prediction from analysis of a combined HIV-COVID-19 co-infection model via ABC-fractional operator, *Alex. Eng. J.,* **60** (2021), 2979–2995. https://doi.org/10.1016/j.aej.2021.01.041

21. R. Hilfer, Applications of fractional calculus in physics, World scientific, 2000.

22. E. M. Lotfi, H. Zine, D. F. M. Torres, N. Yousfi, The power fractional calculus: First definitions and properties with applications to power fractional differential equations, *Mathematics,* **10** (2022), 3594. https://doi.org/10.3390/math10193594

23. G. Boeing, Visual analysis of nonlinear dynamical systems: chaos, fractals, self-similarity and the limits of prediction, *Systems,* **4** (2016), 37. https://doi.org/10.3390/systems4040037

24. T. K. Debnath, The effect of chaos theory in the field of business: A review, *Int. J. Prog. Res. Sci. Eng.,* **3** (2022), 88–92.

25. A. Hastings, C. L. Hom, S. Ellner, P. Turchin, H. C. J. Godfray, Chaos in ecology: is mother nature a strange attractor?, *Annu. Rev. Ecol. S.,* 1993, 1–33.

26. R. G. L. Pryor, J. E. H. Bright, Chaos, complexity and COVID-19: The chaos theory of careers in 2022, *Aust. J. Career Dev.,* **31** (2022), 201–205. https://doi.org/10.1177/10384162221120710

27. D. Rickles, P. Hawe, A. Shiell, A simple guide to chaos and complexity, *J. Epidemiol. Commun. H.,* **61** (2007), 933–937. https://doi.org/10.1136/jech.2006.054254

28. J. M. Ginoux, R. Meucci, J. Llibre, J. C. Sprott, *The jerk dynamics of Lorenz model*, In: International Conference on Nonlinear Dynamics and Applications, Springer, 2023, 121–129. https://doi.org/10.1007/978-3-031-50635-2_12

29. E. N. Lorenz, Deterministic nonperiodic flow, *J. Atmos. Sci.,* **20** (1963), 130–141.

30. T. N. Palmer, E. N. Lorenz, May 1917-16 April 2008 Biogr, *Mems. Fell. R. Soc.,* **55** (2009), 189–205.

31. B. W. Shen, A Review of Lorenz's Models from 1960 to 2008, *Int. J. Bifurcat. Chaos,* **33** (2023), 2330024. https://doi.org/10.1142/S0218127423300240

32. M. S. Larruy, *Chaotic dynamical systems. Applications to engineering and communications*, B.S. thesis, Universitat Politècnica de Catalunya, 2024.

33. M. Borah, A. Gayan, J. S. Sharma, Y. Chen, Z. Wei, V.-T. Pham, Is fractional-order chaos theory the new tool to model chaotic pandemics as Covid-19?, *Nonlinear Dyn.,* **109** (2022), 1187–1215. https://doi.org/10.1007/s11071-021-07196-3
34. A. Fernández-Díaz, Overview and perspectives of chaos theory and its applications in economics, *Mathematics,* **12** (2024), 92. https://doi.org/10.3390/math12010092
35. D. Guegan, Chaos in economics and finance, *Annu. Rev. Control,* **33** (2009), 89–93. https://doi.org/10.1016/j.arcontrol.2009.01.002
36. T. A. Al-Maadeed, I. Hussain, A. Anees, M. T. Mustafa, A image encryption algorithm based on chaotic Lorenz system and novel primitive polynomial S-boxes, *Multimed. Tools App.,* **80** (2021), 24801–24822. https://doi.org/10.1007/s11042-021-10695-5
37. W. Alexan, M. ElBeltagy, A. Aboshousha, Rgb image encryption through cellular automata, s-box and the lorenz system, *Symmetry,* **14** (2022), 443. https://doi.org/10.3390/sym14030443
38. F. Bagnoli, M. Baia, Synchronization, control and data assimilation of the Lorenz system, *Algorithms,* **16** (2023), 213. https://doi.org/10.3390/a16040213
39. N. Stankevich, Stabilization and complex dynamics initiated by pulsed force in the Rössler system near saddle-node bifurcation, *Nonlinear Dyn.,* **112** (2024), 2949–2967. https://doi.org/10.1007/s11071-023-09183-2
40. N. Kuznetsov, T. Mokaev, V. Ponomarenko, E. Seleznev, N. Stankevich, L. Chua, Hidden attractors in Chua circuit: Mathematical theory meets physical experiments, *Nonlinear Dyn.,* **111** (2023), 5859–5887. https://doi.org/10.1007/s11071-022-08078-y
41. X. Zhang, C. Li, A novel type of chaotic attractor with a multiunit structure: From multiscroll attractors to multi-bond orbital attractors, *Eur. Phys. J. Plus,* **137** (2022), 1048. https://doi.org/10.1353/mln.2022.0076
42. A. Dlamini, E. F. D. Goufo, M. Khumalo, On the Caputo-Fabrizio fractal fractional representation for the Lorenz chaotic system, *AIMS Math.,* **6** (2021), 12395–12421. http://dx.doi.org/10.3934/math.2021717
43. A. Dlamini, E. F. D. Goufo, M. Khumalo, Strongly perturbed bondorbital attractors for generalized systems, *Chaos,* **35** (2025). https://doi.org/10.1063/5.0249237
44. S. Saber, Control of Chaos in the Burke-Shaw system of fractal-fractional order in the sense of Caputo-Fabrizio, *J. Appl. Math. Comput. Mech.,* **23** (2024), 83–96. https://doi.org/10.17512/jamcm.2024.1.07
45. N. Almutairi, S. Saber, On chaos control of nonlinear fractional Newton-Leipnik system via fractional Caputo-Fabrizio derivatives, *Sci. Rep.,* **13** (2023), 22726. https://doi.org/10.1038/s41598-023-49541-z
46. A. M. Alqahtani, S. Sharma, A. Chaudhary, A. Sharma, Application of Caputo-Fabrizio derivative in circuit realization, *AIMS Math.,* **10** (2025), 2415–2443. https://dx.doi.org/10.3934/math.2025113
47. A. I. Arik, I. S. Araz, Delay differential equations with fractional differential operators: Existence, uniqueness and applications to chaos, *Commun. Anal. Mech.,* **16** (2024), 169–192. http://dx.doi.org/10.3934/cam.2024008

48. Y. Şahin, M. Merdan, New numerical solutions for Caputo–Fabrizio fractional differential multidimensional diffusion problems, *Int. J. Math. Math. Sci.,* **2025** (2025), 5554516. https://doi.org/10.1155/ijmm/5554516

49. S. M. S. Rana, M. J. Uddin, A. Q. Khan, Bifurcation and chaos in a discrete fractional order reduced Lorenz model with Caputo and conformable derivatives, *J. Appl. Anal. Comput.,* **15** (2025), 1241–1271. https://doi.org/10.11948/20240181

50. P. A. Glendinning, D. J. W. Simpson, Robust chaos and the continuity of attractors, *Trans. Math. Appl.,* **4** (2020), tnaa002. https://doi.org/10.1093/imatrm/tnaa002

51. C. Letellier, L. F. Olsen, S. Mangiarotti, Chaos: From theory to applications for the 80th birthday of Otto E. Rössler, *Chaos,* **31** (2021). https://doi.org/10.1063/5.0058332

52. F. Li, J. Zeng, Multi-scroll attractor and multi-stable dynamics of a three-dimensional jerk system, *Energies,* **16** (2023), 2494. https://doi.org/10.3390/en16052494

53. Y. Ye, J. He, Constructing a new multi-scroll chaotic system and its circuit design, *Mathematics,* **12** (2024), 1931. https://doi.org/10.3390/math12131931

54. E. Kreyszig, *Introductory functional analysis with applications*, Wiley, 1989.

55. F. Jarad, T. Abdeljawad, Applications of the Caputo–Fabrizio fractional derivative to the modeling of real-world phenomena, *Chaos Soliton. Fract.,* **123** (2019), 275–286. https://doi.org/10.1016/j.urology.2018.04.048

56. K. Diethelm, *The analysis of fractional differential equations*, Springer, 2010.

AIMS Press